



HAL
open science

On 3D DDFV discretization of gradient and divergence operators. II. Discrete functional analysis tools and applications to degenerate parabolic problems.

Boris Andreianov, Mostafa Bendahmane, Florence Hubert

► To cite this version:

Boris Andreianov, Mostafa Bendahmane, Florence Hubert. On 3D DDFV discretization of gradient and divergence operators. II. Discrete functional analysis tools and applications to degenerate parabolic problems.. 2011. hal-00567342v2

HAL Id: hal-00567342

<https://hal.science/hal-00567342v2>

Submitted on 22 Nov 2011 (v2), last revised 22 Apr 2013 (v3)

HAL is a multi-disciplinary open access archive for the deposit and dissemination of scientific research documents, whether they are published or not. The documents may come from teaching and research institutions in France or abroad, or from public or private research centers.

L'archive ouverte pluridisciplinaire **HAL**, est destinée au dépôt et à la diffusion de documents scientifiques de niveau recherche, publiés ou non, émanant des établissements d'enseignement et de recherche français ou étrangers, des laboratoires publics ou privés.

ON 3D DDFV DISCRETIZATION OF GRADIENT AND DIVERGENCE OPERATORS. II. DISCRETE FUNCTIONAL ANALYSIS TOOLS AND APPLICATIONS TO DEGENERATE PARABOLIC PROBLEMS.

B. ANDREIANOV, M. BENDAHMANE, AND F. HUBERT

ABSTRACT. This paper is the sequel of the paper [2] of S. Krell and the authors, where a family of 3D finite volume schemes on “double” meshes was constructed and the crucial discrete duality property was established. Heading towards applications, we state some discrete functional analysis tools (consistency results, Poincaré and Sobolev embedding inequalities, discrete $W^{1,p}$ compactness, discrete L^1 compactness in space and time) for the DDFV scheme of [2]. We apply them to infer convergence of discretizations of nonlinear elliptic-parabolic problems of Leray-Lions kind, and illustrate them with numerical results. Applications to degenerate parabolic-hyperbolic PDEs and to a degenerate parabolic system known in electro-cardiology are briefly discussed.

CONTENTS

1. Introduction	2
2. Notation for 3D CeVe-DDFV scheme, operators and discrete duality	3
2.1. Notation and formulas used in some proofs	4
2.2. An illustration: cartesian DDFV meshes in 3D	5
3. Discrete functional analysis tools	6
3.1. Regularity assumptions on the meshes	6
3.2. Consistency of projections and discrete gradients	7
3.3. Discrete Poincaré inequality, Sobolev embeddings and strong compactness	11
3.4. Discrete $W^{1,p}(\Omega)$ weak compactness	13
3.5. Discrete operators, functions and fields on $(0, T) \times \Omega$	15
3.6. Strong compactness in $L^1((0, T) \times \Omega)$	15
4. Applications and convergence proofs	16
4.1. Leray-Lions elliptic and parabolic problems	16
4.2. A parabolic-elliptic “bidomain” cardiac model	20
4.3. Degenerate convection-diffusion problems and discrete entropy dissipation	21
5. Numerical results for elliptic-parabolic problems	22
6.A. Appendix A: An L^1 space-and-time compactness lemma	24
6.B. Appendix B: A penalization operator	28
6.C. Appendix C: DDFV discretization of reaction terms	29
6.D. Appendix D: The coordination-decomposition algorithm	30
References	31

Date: November 22, 2011.

2000 Mathematics Subject Classification. 65N12, 65M12.

Key words and phrases. Finite volume approximation, Discrete duality, 3D CeVe-DDFV, Convergence, Consistency, Discrete compactness, Discrete Sobolev embeddings, Degenerate parabolic problems.

1. INTRODUCTION

Duality formula linking discrete divergence and discrete gradient operators are a key property for the convergence analysis of many known numerical schemes (cf. [2]). The name of DDFV (Discrete Duality Finite Volume) was given to a particular kind of 2D schemes that possess this duality feature and work on “double” meshes (see Hermeline [40, 42] and references therein; Domelevo and Omnès [25]; cf. Nicolaïdes [45]). The present paper partially follows the guidelines of Andreianov, Boyer and Hubert [10], where the 2D DDFV method was used for discretization of nonlinear diffusion problems. The importance of the discrete duality feature stems from the fact that it makes finite volume discretizations of numerous elliptic operators “structure-preserving” (which means e.g. that the discretization of monotone coercive operators is monotone and coercive).

The goal of this paper is to collect several tools for analysis of DDFV schemes (many of them are straightforward extensions from the 2D case); to illustrate their use in convergence proofs (see also [25, 10, 15, 3, 5, 19] for this purpose); and to illustrate one of the convergence theorems by numerical experiments.

We focus on the 3D DDFV schemes from the works [4, 2] of the authors and Karlsen and Krell. In these works, a 3D generalization of the 2D DDFV scheme, called CeVe-DDFV, was described and the discrete duality property was justified. Our construction coincides with the one given by Hermeline in [42]¹. Other kinds of 3D DDFV schemes are in use. First, a slightly different CeVe-DDFV scheme was designed by Pierre in [47] (see also [24, 22, 23] and [21]). Developing the approach of Hermeline [41] for introducing additional unknowns, a scheme with a different idea for mesh and gradient construction, now called CeVeFE-DDFV, was introduced by Coudière and Hubert in [18, 19], see also [20]. A 3D DDFV construction inspired by [19] was recently proposed in [32]; this construction boils down to a generalization of the scheme of [47]. More information is given in [10].

In Section 2 we recall the basic notation for 3D DDFV schemes, spaces of discrete functions and fields, discrete divergence and discrete gradient operators; the details are given in [2]. The notation reflects the far-reaching analogy between the continuous framework and the discrete DDFV framework, and makes the convergence proofs quite similar to the proofs of structural stability (i.e., of the stability of solutions w.r.t perturbation of data and nonlinearities) in the continuous framework.

In Section 3, we first give consistency results for the mesh projection operators and for the discrete gradient operator. Then, we discuss the discrete Poincaré and Sobolev embeddings for the DDFV schemes, and sketch the proof of the embeddings in the case of the Neumann boundary conditions. We give two kinds of discrete compactness results. The $W^{1,p}$ weak compactness in space is well known in 2D (see in particular [10]). The L^1 space-time compactness is a result of independent interest: its proof (Appendix A) is based upon the original idea of Kruzhkov [44]. In Appendix B, we introduce a penalization operator, helpful in some convergence studies, and in Appendix C we give a hint on discretization of reaction terms in the context of DDFV schemes.

In Section 4 we outline the proof of the convergence of our 3D DDFV discretizations for elliptic and parabolic-elliptic equations with Leray-Lions kind nonlinear diffusion (see Alt and Luckhaus [1]) $b(u)_t - \operatorname{div} \varphi(\nabla u) = f$ with the homogeneous Dirichlet boundary conditions. The arguments of the proof are similar to those of the work [10] of the elliptic case, augmented by specific techniques for time compactness of discrete solutions. A similar study (with, in addition, error estimates like in [10]) for the 3D CeVeFE-DDFV scheme is given in [18], in the elliptic case. We also describe the convergence results obtained in the joint work of two of the authors with Karlsen and Pierre [5] on degenerate parabolic problems coming from applications in electrocardiology (see [5] for numerical results); and we discuss the additional tools needed for degenerate hyperbolic-parabolic problems coming from sedimentation applications ([3]).

In Section 5, we report on numerical results for both linear and nonlinear equations with Leray-Lions kind diffusion. For related numerical results on convergence of different kinds of 3D DDFV

¹The work [42] imposes unnecessary restrictions on the meshes but it treats the more delicate case of diffusion operators with discontinuous coefficients.

schemes, we refer to Hermeline [41, 42] and Coudière and Hubert [18] (in the context of linear heterogeneous anisotropic diffusion operators) and to Coudière et al. [22, 24, 23] (in the context of electrocardiology). An extended comparison of different schemes on linear 3D diffusion problems will be carried out in the benchmark [38], see in particular [12, 20, 21]. Recall that the problem we solve numerically is a nonlinear one; Appendix D presents the coordination-decomposition iterative algorithm (see [36, 37, 15]) used in the numerical tests of the present paper.

2. NOTATION FOR 3D CEVE-DDFV SCHEME, OPERATORS AND DISCRETE DUALITY

Let us briefly recall our discrete framework, limited to the case of operators with homogeneous Dirichlet or Neumann boundary conditions. The cases of non-homogeneous and mixed boundary conditions are treated in [10] and in [5].

We only reproduce the notation needed to understand the statements of the paper and the applications in Section 4. Illustrative figures and additional notation that is only needed in some proofs of Section 3 are given without comment in Section 2.1 (for details, see the paper [2] of the authors and S. Krell).

DDFV schemes are designed for discretization in space of second-order elliptic operators in divergence form; therefore we concentrate on description of the meshes of a domain $\Omega \subset \mathbb{R}^3$ (notation related to the time dependence is given in Section 3.5). The 3D CeVe-DDFV meshes of Ω described in [2, 12] (cf. [4] and Hermeline [42]) are triples $\mathfrak{T} = (\overline{\mathfrak{M}}^o, \overline{\mathfrak{M}}^*, \mathfrak{D})$; actually both $\overline{\mathfrak{M}}^*$ and \mathfrak{D} are constructed from $\overline{\mathfrak{M}}^o$ which is given.

The mesh \mathfrak{T} consists of control volumes of two kinds, the primal ones (denoted $K \in \overline{\mathfrak{M}}^o$) and the dual ones (denoted $K^* \in \overline{\mathfrak{M}}^*$). Both primal and dual volumes form a partition of Ω , up to a set of measure zero. The volumes are associated with centers x_K and x_{K^*} , respectively; one may assume that $x_K \in K$ and $x_{K^*} \in K^*$. The dual volumes are constructed using, as vertices, the primal volume centers $(x_K)_K$, some face centers $(x_{K|L})_{K|L}$ ($K|L$ being the notation for a face separating neighbours K and L) and the edge middlepoints $(x_{K^*|L^*})_{K^*|L^*}$ (K^* and L^* being neighbour dual centers), see [2, Sec. 2] for details; cf. [42].

The dual and primal volumes with centers lying on $\partial\Omega$ are considered as “boundary” volumes (denoted $K \in \partial\overline{\mathfrak{M}}^o$ and $K^* \in \partial\overline{\mathfrak{M}}^*$, resp.), in the case we look at Dirichlet boundary conditions. The primal boundary volumes are in fact fictive ones (they are flat: each face of $K \in \overline{\mathfrak{M}}^o$ contained in $\partial\Omega$ gives rise to a boundary volume). With each (primal or dual) interior control volume (denoted $K \in \overline{\mathfrak{M}}^o$ or $K^* \in \overline{\mathfrak{M}}^*$, resp.), unknown values u_K , resp. u_{K^*} for a discrete solution u are associated (the value u_K , resp. u_{K^*} , is seen as the value of u at the point x_K , resp. x_{K^*}); Dirichlet boundary conditions are imposed at the centers of the boundary volumes. The Neumann or Robin boundary conditions, when present, enter the definition of the discrete divergence operator near the boundary (see [16, 43] and [5] for details).

Thus we consider the space $\mathbb{R}^\mathfrak{T}$ of discrete functions on interior volumes; a discrete function $u^\mathfrak{T} \in \mathbb{R}^\mathfrak{T}$ consists of one real value per primal or dual interior control volume. The space of discrete functions that take the value zero in the boundary volumes is denoted by $\mathbb{R}_0^\mathfrak{T}$; more generally, by $u^\mathfrak{T} \in \mathbb{R}^\mathfrak{T}$ we mean the extension of $u^\mathfrak{T} \in \mathbb{R}^\mathfrak{T}$ by values assigned in boundary volumes. On $\mathbb{R}^\mathfrak{T}$, one considers the appropriate product $\left[\cdot, \cdot \right]_\Omega$ (see formula (2) below) which is a bilinear positive form.

The couples of neighbour primal and dual volumes define a partition of Ω into diamonds (denoted $D \in \mathfrak{D}$), used to represent discrete gradients and other discrete fields on Ω . A diamond D is uniquely determined by a couple K, L of primal volumes that have common interface $K|L$ contained within D ; in this case, we denote it $D^{K|L}$ (see [2, Sec. 4] for several generalizations). Diamonds are further cut into subdiamonds, denoted $s_{K^*|L^*}^{K|L}$ (or $s \in \mathfrak{S}$, for a generic subdiamond) that involve neighbours K, L and dual neighbours K^*, L^* intersecting K, L (see Fig. 1); these are only needed inside some proofs of Section 3. The space $(\mathbb{R}^\mathfrak{D})^3$ of discrete fields on Ω serves to define the fluxes through the boundaries of control volumes. A discrete field $\vec{\mathcal{F}}^\mathfrak{T} \in (\mathbb{R}^\mathfrak{D})^3$ on Ω consists of one \mathbb{R}^3 value per diamond. On $(\mathbb{R}^\mathfrak{D})^3$, one considers the appropriate scalar product $\left\{ \cdot, \cdot \right\}_\Omega$ (see formula (3) below).

A Discrete Duality Finite Volume scheme is determined by the mesh, the discrete divergence operator $\operatorname{div}^\varepsilon : (\mathbb{R}^\mathfrak{D})^3 \rightarrow \mathbb{R}^\varepsilon$ (see formula (4) below) obtained by the standard finite volume discretization procedure (taking into account the Neumann or Robin boundary condition, if necessary), and by the associated discrete gradient operator $\nabla^\varepsilon : \mathbb{R}^\varepsilon \rightarrow (\mathbb{R}^\mathfrak{D})^3$ (see formula (5) below) obtained diamond-wise, by a kind of affine interpolation (see [2] for the motivation behind the definition of ∇^ε). The essential property of the DDFV schemes is the discrete duality [2, Prop.3.2] (cf. [42, Th.1]), stated as

$$(1) \quad \left[-\operatorname{div}^\varepsilon \vec{\mathcal{F}}^\varepsilon, v^\varepsilon \right]_\Omega = \left\{ \vec{\mathcal{F}}^\varepsilon, \nabla^\varepsilon v^\varepsilon \right\}_\Omega;$$

this form is suitable either for v satisfying the homogeneous Dirichlet boundary condition, or for $\vec{\mathcal{F}}$ satisfying the homogeneous Neumann (zero-flux) boundary condition (see [5, 43] for the general case including a boundary scalar product).

The discrete solution u^ε will be often identified with the piecewise constant function

$$u^\varepsilon := \frac{1}{3} v^{\mathfrak{m}^\circ} + \frac{2}{3} v^{\mathfrak{m}^*}$$

with $v^{\mathfrak{m}^\circ}$ and $v^{\mathfrak{m}^*}$ representing the piecewise constant discrete solutions on the primal and the dual mesh, respectively; e.g., $v^{\mathfrak{m}^\circ}(x) = \sum_{K \in \mathfrak{m}^\circ} v_K \mathbb{1}_K(x)$. Similarly, we identify $\nabla^\varepsilon u^\varepsilon$ with the piecewise constant function $\nabla^\varepsilon u^\varepsilon := \sum_{D \in \mathfrak{D}} \nabla_D u^\varepsilon \mathbb{1}_D(x)$. This identification is related to the notion of reconstruction (lifting) operator used in the context of “gradient schemes”, see Eymard, Herbin and Guichard [32].

We denote by $\operatorname{Vol}(A)$ the three-dimensional Lebesgue measure of A which can stand for a control volume, a dual control volume, a diamond, etc.

2.1. Notation and formulas used in some proofs. For the sake of self-consistency, let us reproduce some figures and formulas from [2] used in the proofs of Section 3.

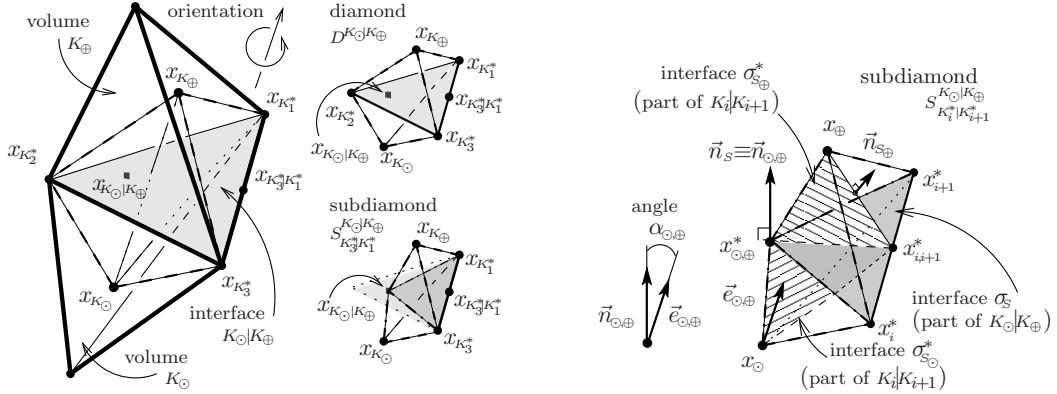


FIGURE 1. 3D neighbour volumes, diamond, subdiamond. Zoom on a subdiamond.

For $w^\varepsilon, v^\varepsilon \in \mathbb{R}^\varepsilon$ and for $\vec{\mathcal{F}}^\varepsilon, \vec{\mathcal{G}}^\varepsilon \in (\mathbb{R}^3)^\mathfrak{D}$, the scalar products are given by

$$(2) \quad \left[w^\varepsilon, v^\varepsilon \right]_\Omega = \frac{1}{3} \sum_{K \in \mathfrak{m}^\circ} \operatorname{Vol}(K) w_K v_K + \frac{2}{3} \sum_{K^* \in \mathfrak{m}^*} \operatorname{Vol}(K^*) w_{K^*} v_{K^*};$$

$$(3) \quad \left\{ \vec{\mathcal{F}}^\varepsilon, \vec{\mathcal{G}}^\varepsilon \right\}_\Omega = \sum_{D \in \mathfrak{D}} \operatorname{Vol}(D) \vec{\mathcal{F}}_D \cdot \vec{\mathcal{G}}_D.$$

The entries of the discrete divergence of a field \mathcal{F} are given by

$$(4) \quad \begin{aligned} \operatorname{div}_K \vec{\mathcal{F}}^\varepsilon &= \frac{1}{\operatorname{Vol}(K)} \sum_{S \sim K} m_S \vec{\mathcal{F}}_S \cdot (-1)^{\epsilon_S^K} \vec{n}_S, \\ \operatorname{div}_{K^*} \vec{\mathcal{F}}^\varepsilon &= \frac{1}{\operatorname{Vol}(K^*)} \sum_{S \sim K^*} \vec{\mathcal{F}}_S \cdot (-1)^{\epsilon_S^{K^*}} (m_{S_\ominus}^* \vec{n}_{S_\ominus}^* + m_{S_\oplus}^* \vec{n}_{S_\oplus}^*) \end{aligned}$$

where “ \sim ” means that the subdiamond s is associated with the primal volume κ (resp. with the dual volume κ^*); further, $\epsilon_s^K, \epsilon_s^{K^*}$ are sign selectors such that $(-1)^{\epsilon_s^K} \vec{n}_s$ is the unit normal vector to the part σ_s of $\kappa|L$ that points outside κ , and $(-1)^{\epsilon_s^{K^*}} \vec{n}_s^*$, $(-1)^{\epsilon_s^{K^*}} \vec{n}_{s\oplus}^*$ are the unit normal vectors to the two planar parts $\sigma_{s\ominus}^*, \sigma_{s\oplus}^*$ of $\kappa^*|L^*$ that point outside κ^* .

The entries of the discrete gradient are calculated by the formula

$$(5) \quad \nabla_D w^{\vec{x}} = \frac{1}{6 \text{Vol}(D)} \sum_{i=1}^l \left\{ \frac{\langle \overrightarrow{x_{\ominus} x_{\oplus}}, \overrightarrow{x_{\ominus} x_{\oplus}^*}, \overrightarrow{x_{i+1}^* x_{i+1}} \rangle}{\overrightarrow{x_{\ominus} x_{\oplus}} \cdot \vec{n}_{\ominus, \oplus}} (w_{\oplus} - w_{\ominus}) \vec{n}_{\ominus, \oplus} + 2(w_{i+1}^* - w_i^*) [\overrightarrow{x_{\ominus} x_{\oplus}} \times \overrightarrow{x_{\ominus} x_{\oplus}^*}] \right\}$$

with the notation of Fig. 1 (the depicted case corresponds to primal interface $\kappa_{\ominus}|\kappa_{\oplus}$ with $l = 3$ vertices, with the convention “ $l + 1 := 1$ ”); in (5), $\cdot \cdot \cdot$ and $\langle \cdot, \cdot, \cdot \rangle$ denote the vector and the mixed products of vectors of \mathbb{R}^3 , respectively.

2.2. An illustration: cartesian DDFV meshes in 3D. We reproduce the simple yet important example of a 3D DDFV mesh given in [2].

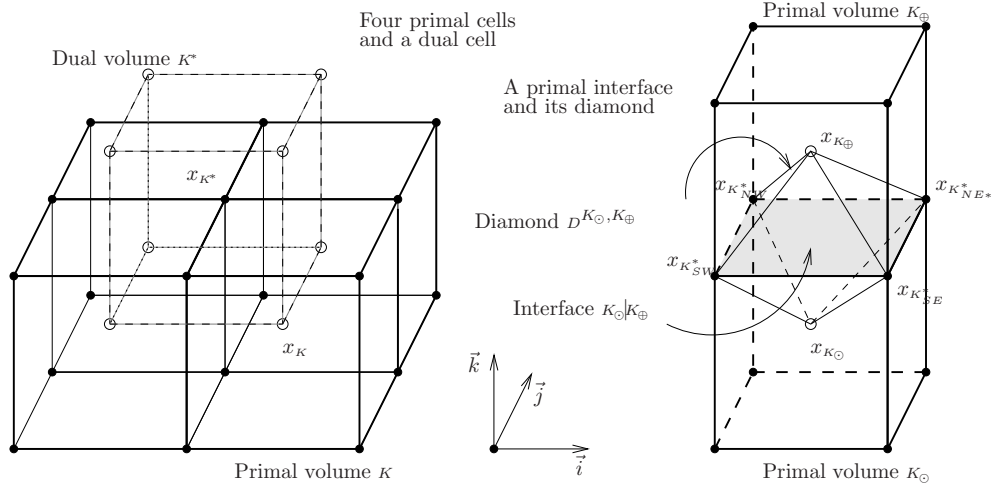


FIGURE 2. Cartesian DDFV mesh in 3D and an associated diamond

Take the unit cube $\Omega = [0, 1]^3$ and partition it into N^3 primal cubic volumes of edge $\frac{1}{N}$. The diamonds are octahedrons built on two primal cubes' centers $x_{\kappa_{\ominus}}, x_{\kappa_{\oplus}}$ and on the square interface $\kappa_{\ominus}|\kappa_{\oplus}$ between them. One chooses for $x_{\kappa_{\ominus}|\kappa_{\oplus}}$ the center of symmetry of $\kappa_{\ominus}|\kappa_{\oplus}$. The interior dual volumes are also cubes of the same edge $\frac{1}{N}$ centered at the vertices of the primal mesh that do not lie on $\partial\Omega$.

To give the entries of the associated discrete gradient, for the sake of being definite we consider a diamond $D = D^{\kappa_{\ominus}|\kappa_{\oplus}}$ with orientation and notation of Fig. 2. Applying the reconstruction formula for discrete gradient (5) (see also [2]) one finds that the entry $\nabla_D w^{\vec{x}}$ of $\nabla^{\vec{x}} w^{\vec{x}}$ is computed as

$$\nabla_D w^{\vec{x}} = \frac{1}{2} \left(\frac{w_{\kappa_{NE}^*} - w_{\kappa_{NW}^*}}{1/N} + \frac{w_{\kappa_{SE}^*} - w_{\kappa_{SW}^*}}{1/N} \right) \vec{i} + \frac{1}{2} \left(\frac{w_{\kappa_{NE}^*} - w_{\kappa_{SE}^*}}{1/N} + \frac{w_{\kappa_{NW}^*} - w_{\kappa_{SW}^*}}{1/N} \right) \vec{j} + \frac{w_{\kappa_{\oplus}} - w_{\kappa_{\ominus}}}{1/N} \vec{k};$$

here the triple $(\vec{i}, \vec{j}, \vec{k})$ denotes the canonical basis of \mathbb{R}^3 . For later use, notice that the most convenient orthonormal basis for expressing $\nabla_D w^{\vec{x}}$ is $(\frac{\vec{i} + \vec{j}}{\sqrt{2}}, \frac{\vec{j} - \vec{i}}{\sqrt{2}}, \vec{k})$; accordingly, we find

$$(6) \quad |\nabla_D w^{\vec{x}}|^2 = \left| \frac{w_{\kappa_{NE}^*} - w_{\kappa_{SW}^*}}{\sqrt{2}/N} \right|^2 + \left| \frac{w_{\kappa_{NW}^*} - w_{\kappa_{SE}^*}}{\sqrt{2}/N} \right|^2 + \left| \frac{w_{\kappa_{\oplus}} - w_{\kappa_{\ominus}}}{1/N} \right|^2.$$

Further, let κ be an interior primal volume. For the six diamonds that intersect κ , we introduce the specific notation $D_{\text{abv}}(\kappa), D_{\text{blw}}(\kappa), D_{\text{E}}(\kappa), D_{\text{W}}(\kappa)$ and $D_{\text{N}}(\kappa), D_{\text{S}}(\kappa)$ with the obvious meaning of the subscripts (e.g., the diamond pictured on the right in Figure 2 is $D_{\text{blw}}(\kappa_{\oplus})$ and at the same time, it is $D_{\text{abv}}(\kappa_{\ominus})$).

Applying the formula for the discrete divergence (4) (see also [2]) one finds that the entry $\operatorname{div}_K \vec{\mathcal{F}}^{\vec{x}}$ of $\operatorname{div}^{\vec{x}} \vec{\mathcal{F}}^{\vec{x}}$ is computed as

$$\operatorname{div}_K \vec{\mathcal{F}}^{\vec{x}} = \frac{1}{1/N^3} \left\{ \frac{1}{N^2} (\vec{\mathcal{F}}_{DE(K)} - \vec{\mathcal{F}}_{DW(K)}) \cdot \vec{i} + \frac{1}{N^2} (\vec{\mathcal{F}}_{DN(K)} - \vec{\mathcal{F}}_{DS(K)}) \cdot \vec{j} + \frac{1}{N^2} (\vec{\mathcal{F}}_{Dabv(K)} - \vec{\mathcal{F}}_{Dblw(K)}) \cdot \vec{k} \right\}.$$

The formula for the entries of $\operatorname{div}_{K^*} \vec{\mathcal{F}}^{\vec{x}}$ has an entirely similar form.

3. DISCRETE FUNCTIONAL ANALYSIS TOOLS

In this section, we give a few “discrete functional analysis tools” related to CeVe-DDFV schemes (such properties or their analogues also hold for 2D DDFV schemes and for 3D CeVeFE-DDFV schemes). Notice that the proof of the asymptotic discrete compactness property of Proposition 3.9 is based upon the discrete duality; the duality is also used, in a much weaker form, in the proof of Proposition 3.11. This section is essentially self-contained; some details are given in references [6, 10, 29], notation is taken from Section 2.1 and [2], and one longer proof is postponed to the Appendix A. In addition, two hints on DDFV discretization (namely, the penalization operator and a structure-preserving discretization of the reaction terms) that may be useful for coping with “double” nature of the CeVe-DDFV approximations are postponed to Appendices B and C.

For a given mesh \mathfrak{T} of Ω as described in [2, Sec. 2] (see also [2, Sec. 4]), the size of \mathfrak{T} is defined as

$$\operatorname{size}(\mathfrak{T}) := \max \left\{ \max_{K \in \mathfrak{M}^{\mathfrak{T}}} \operatorname{diam}(K), \max_{K^* \in \mathfrak{M}^{\mathfrak{T}*}} \operatorname{diam}(K^*), \max_{D \in \mathfrak{D}} \operatorname{diam}(D) \right\}.$$

If the assumption $x_K \in K$ made in [2, Sec. 2] is dropped (see [2, Sec. 4]), then in the above expression $\operatorname{diam}(K)$ should be replaced with the diameter of the convex hull of K and x_K .

In what follows, we will always think of a family of meshes such that $\operatorname{size}(\mathfrak{T})$ goes to zero.

3.1. Regularity assumptions on the meshes.

In various finite volume methods, one always needs some qualitative restrictions on each mesh \mathfrak{T} considered (such as, e.g., the assumption that $x_K \in K$, or the convexity of volumes and/or diamonds, or the mesh orthogonality, or the Delaunay condition on a simplicial mesh). For the convergence analysis on families of such meshes, it is convenient (though not always necessary) to impose shape regularity assumptions on the family of meshes considered. These assumptions are quantitative: this means that the “distortion” of certain objects in a mesh is measured with the help of a regularity constant $\operatorname{reg}(\mathfrak{T})$, which is finite for each individual mesh but may get unbounded if an infinite family of meshes is considered.

For the 3D DDFV meshes presented in this paper, there are two main mesh regularity assumptions. First, we require several lower bounds on $d_{KL} = |x_K - x_L|$, $d_{K^*L^*} = |x_{K^*} - x_{L^*}|$:

$$(7) \quad \left\{ \begin{array}{l} \text{For all primal neighbours } K, L, \quad \operatorname{diam}(K) + \operatorname{diam}(L) \leq \operatorname{reg}(\mathfrak{T}) d_{KL}; \\ \text{for all dual neighbours } K^*, L^*, \quad \operatorname{diam}(K^*) + \operatorname{diam}(L^*) \leq \operatorname{reg}(\mathfrak{T}) d_{K^*L^*}; \\ \text{for all diamond } D \text{ with vertices } x_K, x_L \\ \text{and with neighbour dual vertices } x_{K^*}, x_{L^*}, \quad \operatorname{diam}(D) \leq \operatorname{reg}(\mathfrak{T}) \min\{d_{KL}, d_{K^*L^*}\}. \end{array} \right.$$

Further, we need a bound on the inclination of the (primal and dual) interfaces with respect to the (dual or primal) edges (see Fig. 1):

$$(8) \quad \left\{ \begin{array}{l} \text{For all primal neighbour volumes } K, L, \text{ the angle } \alpha_{K,L} \text{ between } \overrightarrow{x_K x_L} \text{ and the plane } K \setminus L \\ \text{is separated from } 0 \text{ and } \pi, \text{ meaning that } \operatorname{reg}(\mathfrak{T}) \cos \alpha_{K,L} \geq 1; \\ \text{and for all neighbour vertices } x_{K^*}, x_{L^*} \text{ of } K \setminus L, \\ \text{the angle } \alpha_{K^*,L^*}^* \text{ between } \overrightarrow{x_{K^*} x_{L^*}} \text{ and } \overrightarrow{x_{K^*|L^*} x_{K|L}} \\ \text{is separated from } 0 \text{ and } \pi, \text{ namely } \operatorname{reg}(\mathfrak{T}) \cos \alpha_{K^*,L^*}^* \geq 1. \end{array} \right.$$

Also a uniform bound on the number of neighbours of volumes and diamonds is useful:

$$(9) \quad \left\{ \begin{array}{l} \text{All primal volume } K \text{ has at most } \operatorname{reg}(\mathfrak{T}) \text{ neighbour primal volumes;} \\ \text{all dual volume } K^* \text{ has at most } \operatorname{reg}(\mathfrak{T}) \text{ neighbour dual volumes;} \\ \text{and all diamond } D \text{ has at most } \operatorname{reg}(\mathfrak{T}) \text{ vertices.} \end{array} \right.$$

The last line in (9) is satisfied, e.g., if one works either with meshes where all primal interfaces are triangles (thus any diamond has five vertices), or with the uniform cartesian mesh of Section 2.2. Indeed, when the number l of vertices of a face $\kappa|L$ exceeds three, the kernel of the linear form used to reconstruct the discrete gradient in $D^{\kappa|L}$ (see (5) and [2]) is not reduced to discrete functions constant at the vertices of $\kappa|L$. This is a problem e.g. for the discrete Poincaré inequality and for the proof of discrete compactness. In general, the situation with $l \leq 4$ vertices is not clear; e.g. the discrete Poincaré inequality holds on every individual mesh, but it is not an easy task to prove that the embedding constant is uniform, even under rigid proportionality assumptions on the meshes. The uniform cartesian meshes is one case with $l = 4$ that can be treated thoroughly. From the numerical point of view, higher values of l do not lead to troubles for the test cases we have examined (see, e.g., [2, Sec. 5]).

For the Sobolev embedding inequalities and for strong compactness in L^q , $q > 1$, we also require

$$(10) \quad \left\{ \begin{array}{l} \text{For all primal volume } \kappa \text{ and interface } \kappa|L, \quad m_{\kappa|L} d_{\kappa L} \leq \text{reg}(\mathfrak{T}) \text{Vol}(\kappa); \\ \text{For all dual volume } \kappa \text{ and interface } \kappa^*|L^*, \quad m_{\kappa^*|L^*} d_{\kappa^* L^*} \leq \text{reg}(\mathfrak{T}) \text{Vol}(\kappa^*). \end{array} \right.$$

Whenever one is interested in error rate analysis, further constraints on the shape of volumes, dual volumes, diamonds, and their intersections are needed (see [10] for the 2D case). In the 3D case, shape-regularity constraints on the faces of primal and dual meshes would also be required.

3.2. Consistency of projections and discrete gradients. Here we gather basic consistency results for the DDFV discretizations. Heuristically, for a given function φ on Ω , projection of φ on a mesh \mathfrak{T} and subsequent application of the discrete gradient $\nabla^{\mathfrak{T}}$ should produce a discrete field sufficiently close (as $\text{size}(\mathfrak{T})$ gets small) to $\nabla\varphi$. Similarly, for a given field $\vec{\mathcal{F}}$, the adequate projection on the mesh and the application of $\text{div}^{\mathfrak{T}}$ to this projection should yield a discrete function close to $\text{div}\vec{\mathcal{F}}$. Actually, we state two different kinds of consistency results, those in a norm and those in a weaker formulation using duality.

We use two kinds of projection, the mean-value and the center-value ones. Namely, for scalar functions on Ω , the following projections on $\mathbb{R}^{\mathfrak{T}}$ (which have two components, namely the projections on \mathfrak{M}° and on \mathfrak{M}^*) are used:

$$\begin{aligned} \mathbb{P}^{\mathfrak{T}} : \varphi &\mapsto \left(\left(\frac{1}{\text{Vol}(K)} \int_K \varphi \right)_{K \in \mathfrak{M}^{\circ}}, \left(\frac{1}{\text{Vol}(K^*)} \int_{K^*} \varphi \right)_{K^* \in \mathfrak{M}^*} \right) =: \left(\mathbb{P}^{\mathfrak{M}^{\circ}} \varphi, \mathbb{P}^{\mathfrak{M}^*} \varphi \right), \\ \mathbb{P}_c^{\mathfrak{T}} : \varphi &\mapsto \left(\left(\varphi(x_K) \right)_{K \in \mathfrak{M}^{\circ}}, \left(\varphi(x_{K^*}) \right)_{K^* \in \mathfrak{M}^*} \right) =: \left(\mathbb{P}_c^{\mathfrak{M}^{\circ}} \varphi, \mathbb{P}_c^{\mathfrak{M}^*} \varphi \right). \end{aligned}$$

If, in addition, φ is zero on $\partial\Omega$, then $\mathbb{P}_c^{\mathfrak{T}}\varphi \in \mathbb{R}^{\mathfrak{T}}$ is extended to $\mathbb{P}_c^{\overline{\mathfrak{T}}}\varphi \in \mathbb{R}_0^{\overline{\mathfrak{T}}}$; $\mathbb{P}_c^{\overline{\mathfrak{T}}}\varphi$ is the projection of φ on $\mathbb{R}^{\overline{\mathfrak{T}}}$. For \mathbb{R}^3 -valued fields on Ω , we use the projection on $(\mathbb{R}^3)^{\mathfrak{D}}$ by

$$\vec{\mathbb{P}}^{\mathfrak{T}} : \vec{\mathcal{F}} \mapsto \left(\frac{1}{\text{Vol}(D)} \int_D \vec{\mathcal{F}} \right)_{D \in \mathfrak{D}}.$$

Let us stress that for the study of weak compactness in Sobolev spaces and analysis of convergence of discrete solutions to a weak solution of PDEs, the consistency results can be formulated for source terms and for test functions only (and the consistency for $\text{div}^{\mathfrak{T}} \circ \vec{\mathbb{P}}^{\mathfrak{T}}$ is formulated in a weak form, except on very symmetric meshes). These results are shown under the regularity restrictions (7),(8),(9) on the mesh.

Proposition 3.1. *Let \mathfrak{T} be a 3D CeVe-DDFV mesh of Ω as described in [2, Sec. 2.4]. Let $\text{reg}(\mathfrak{T})$ measure the mesh regularity in the sense (7),(8),(9). Then*

(i) *For all $\varphi \in \mathcal{D}(\overline{\Omega})$ one has*

$$\|\varphi - \mathbb{P}^{\mathfrak{M}^{\circ}}\varphi\|_{L^\infty(\Omega)} \leq C(\varphi) \text{size}(\mathfrak{T}), \quad \|\varphi - \mathbb{P}^{\mathfrak{M}^*}\varphi\|_{L^\infty(\Omega)} \leq C(\varphi) \text{size}(\mathfrak{T});$$

²In this paper, we only discuss DDFV discretizations of diffusion operators supplied with homogeneous Dirichlet or Neumann BC. In the homogeneous Dirichlet case, the boundary values of a discrete function are zero. In the homogeneous Neumann case, boundary values never appear. Consideration of non-homogeneous boundary conditions is a highly technical issue. We refer to the analysis of [10] for the Dirichlet case, and to [16, 43, 5] for the non-homogeneous Neumann condition on a part of the boundary.

analogous properties hold for $\mathbb{P}_c^{\mathfrak{M}^o}, \mathbb{P}_c^{\mathfrak{M}^*}$. Similarly, for all $\vec{\mathcal{F}} \in (\mathcal{D}(\overline{\Omega}))^3$ one has

$$\|\vec{\mathcal{F}} - \mathbb{P}^{\mathfrak{T}}\vec{\mathcal{F}}\|_{L^\infty(\Omega)} \leq C(\vec{\mathcal{F}}) \text{size}(\mathfrak{T}).$$

(ii) For all $\varphi \in \mathcal{D}(\Omega)$ one has

$$\|\nabla\varphi - \nabla^{\mathfrak{T}}(\mathbb{P}_c^{\mathfrak{T}}\varphi)\|_{L^\infty(\Omega)} \leq C(\varphi, \text{reg}(\mathfrak{T})) \text{size}(\mathfrak{T}).$$

(iii) Assume that all primal interface $K|L$ is a triangle.

Then for all $\vec{\mathcal{F}} \in (\mathcal{D}(\overline{\Omega}))^3$, for all $w^{\mathfrak{T}} \in \mathbb{R}_0^{\mathfrak{T}}$ one has

$$\left| \left[\mathbb{P}^{\mathfrak{T}}(\text{div} \vec{\mathcal{F}}) - \text{div}^{\mathfrak{T}}(\mathbb{P}^{\mathfrak{T}}\vec{\mathcal{F}}), w^{\mathfrak{T}} \right] \right| \leq C(\vec{\mathcal{F}}, \text{reg}(\mathfrak{T})) \text{size}(\mathfrak{T}) \|\nabla^{\mathfrak{T}} w^{\mathfrak{T}}\|_{L^1(\Omega)}.$$

(iii-bis) Let \mathfrak{T} be a uniform cartesian mesh of Section 2.2. Then for all $\vec{\mathcal{F}} \in (\mathcal{D}(\overline{\Omega}))^3$,

$$\|\mathbb{P}^{\mathfrak{T}}(\text{div} \vec{\mathcal{F}}) - \text{div}^{\mathfrak{T}}(\mathbb{P}^{\mathfrak{T}}\vec{\mathcal{F}})\|_{L^\infty(\Omega)} \leq C(\vec{\mathcal{F}}) \text{size}(\mathfrak{T}).$$

Remark 3.2.

(i) One can perceive (iii),(iii-bis) as a kind of commutation relation, but actually these items also express consistency results. Indeed, by (i), $\mathbb{P}^{\mathfrak{T}}(\text{div} \vec{\mathcal{F}})$ is $\text{size}(\mathfrak{T})$ -close to $\text{div} \vec{\mathcal{F}}$ in $L^\infty(\Omega)$. Therefore the item (iii) can be interpreted as a $\text{size}(\mathfrak{T})$ -smallness of $(\text{div} \vec{\mathcal{F}} - \text{div}^{\mathfrak{T}}(\mathbb{P}^{\mathfrak{T}}\vec{\mathcal{F}}))$ in the weak-* topology of $W^{-1,\infty}(\Omega) = (W_0^{1,1}(\Omega))^*$. Similarly, the item (iii-bis) means that, for the uniform cartesian mesh, $(\text{div} \vec{\mathcal{F}} - \text{div}^{\mathfrak{T}}(\mathbb{P}^{\mathfrak{T}}\vec{\mathcal{F}}))$ is of order $\text{size}(\mathfrak{T})$ in L^∞ norm.

(ii) The items (iii),(iii-bis) reflect a technical difficulty specific to the DDFV context. Indeed, in the context of finite volume schemes with two-point gradient reconstruction (iii),(iii-bis) holds just with $C = 0$, for an appropriately defined field projection operator. To be specific, instead of the DDFV double mesh \mathfrak{T} consider the primal mesh \mathfrak{M}^o alone. One keeps the same definition for diamonds D^{KL} , but sets $\mathbb{P}^{\mathfrak{M}^o}\vec{\mathcal{F}} = (\frac{1}{m_{KL}} \int_{KL} \vec{\mathcal{F}})_{D^{KL} \in \mathfrak{D}}$. One only looks at the first components of the DDFV operators $\mathbb{P}^{\mathfrak{T}}$ and $\text{div}^{\mathfrak{T}}$ (it is natural to denote them $\mathbb{P}^{\mathfrak{M}^o}$ and $\text{div}^{\mathfrak{M}^o}$, respectively). Then from the Green-Gauss formula it is straightforward that

$$(11) \quad \forall \vec{\mathcal{F}} \in (\mathcal{D}(\overline{\Omega}))^3 \quad \mathbb{P}^{\mathfrak{M}^o}(\text{div}^{\mathfrak{M}^o} \vec{\mathcal{F}}) = \text{div}^{\mathfrak{M}^o}(\mathbb{P}^{\mathfrak{M}^o}\vec{\mathcal{F}}).$$

Because in the DDFV context, for $D = D_{K^*|L^*}^{KL}$, the values $\frac{1}{m_{KL}} \int_{KL} \vec{\mathcal{F}}$ and $\frac{1}{m_{K^*|L^*}} \int_{K^*|L^*} \vec{\mathcal{F}}$ may differ, the analogue of the commutation relation (11) cannot be achieved, whatever definition is chosen for $\mathbb{P}^{\mathfrak{T}}$.

Notice that error analysis for diffusion operators would require consistency properties also for functions φ and fields $\vec{\mathcal{F}}$ in Sobolev spaces; this requires more regularity restrictions on the meshes, and much finer techniques (see e.g. [10]). Here, we only need the following additional property generalizing (i) and applicable to source terms:

Corollary 3.3. *Let $p \in [1, +\infty)$. For all $\varphi \in L^p(\Omega)$ one has*

$$\|\varphi - \mathbb{P}^{\mathfrak{M}^o}\varphi\|_{L^p(\Omega)} \rightarrow 0, \quad \|\varphi - \mathbb{P}^{\mathfrak{M}^*}\varphi\|_{L^p(\Omega)} \rightarrow 0 \text{ as } \text{size}(\mathfrak{T}) \rightarrow 0.$$

PROOF : The proof is a straightforward combination of the density of $\mathcal{D}(\overline{\Omega})$ in $L^p(\Omega)$, of Proposition 3.1(i) and of the uniform boundedness of the projection operators $\mathbb{P}^{\mathfrak{M}^o}, \mathbb{P}^{\mathfrak{M}^*}$ seen as operators from $L^p(\Omega)$ to itself. \square

PROOF OF PROPOSITION 3.1:

(i) The properties are evident from the Lipschitz continuity of φ and of $\vec{\mathcal{F}}$, respectively.

(ii) Here the consistency of the discrete gradient on affine functions, stated in [2, Prop.2.3], is used together with the C^2 regularity of φ . Namely, we compare $\nabla^{\mathfrak{T}}\mathbb{P}^{\mathfrak{T}}\varphi$ to $\nabla\varphi$ diamond-wise. From the regularity assumption (7), it is clear that some $C(\text{reg}(\mathfrak{T}))\text{diam}(D)$ -neighbourhood N_D of a given diamond $D = D^{KL} \in \mathfrak{D}$ contains the two primal volumes K, L and the dual volumes

κ_i^* , $i = 1, \dots, l$, used to reconstruct $\nabla_D \mathbb{P}^{\overline{\mathfrak{T}}} \varphi$. Let w denote the affine Taylor polynomial of φ at some fixed point of D (when D touches the boundary $\partial\Omega$, we pick a point at the boundary and get $w \equiv 0$). Then

$$\|\nabla\varphi - \nabla w\|_{L^\infty(D)} \leq C(\varphi)\text{size}(\mathfrak{T}), \quad |\varphi_K - w_K|, |\varphi_L - w_L|, |\varphi_{\kappa_i^*} - w_{\kappa_i^*}| \leq C(\varphi)(\text{diam}(D))^2,$$

where $\varphi_K, \varphi_{\kappa_i^*}$, etc. denote the entries of the discrete function $\mathbb{P}_c^{\overline{\mathfrak{T}}} \varphi$, while $w_K := w(x_K)$, $w_{\kappa_i^*} := w(x_{\kappa_i^*})$ are the values of $\mathbb{P}_c^{\overline{\mathfrak{T}}} w$.

From [2, Prop.2.3], the values $\nabla_D w^{\overline{\mathfrak{T}}}$ and $\nabla w|_D$ coincide. In order to estimate the difference $\|\nabla\varphi - \nabla^{\overline{\mathfrak{T}}}(\mathbb{P}^{\overline{\mathfrak{T}}}\varphi)\|_{L^\infty(D)}$, it remains to compare the values $\nabla_D w^{\overline{\mathfrak{T}}}$ and $\nabla_D(\mathbb{P}^{\overline{\mathfrak{T}}}\varphi)$. Notice that thanks to the previous $(\text{diam}(D))^2$ bounds on $|\varphi_K - w_K|$, $|\varphi_L - w_L|$ and to the bound $\text{reg}(\mathfrak{T})d_{KL} \geq \text{diam}(D)$ in (7), we have

$$\left| \frac{w_L - w_K}{d_{KL}} - \frac{\varphi_L - \varphi_K}{d_{KL}} \right| \leq C(\text{reg}(\mathfrak{T})) \text{diam}(D) \leq C(\text{reg}(\mathfrak{T})) \text{size}(\mathfrak{T}).$$

In view of the expression of the discrete gradient (formula (5) and [2, form. (4),(5)]) and in view of the mesh inclination bound (8) (notice that $\cos\alpha_{K,L}$ appears in the denominator of formula (5)), the contribution of the values in K, L into $|\nabla_D w^{\overline{\mathfrak{T}}} - \nabla_D(\mathbb{P}^{\overline{\mathfrak{T}}}\varphi)|$ is estimated by $C(\text{reg}(\mathfrak{T})) \text{size}(\mathfrak{T})$. Looking closely at the Proj_D^* component in formula [2, form. (4),(5)] (notice in particular that $\cos\alpha_{\kappa_i^*, \kappa_{i+1}^*}$ appears in the denominator, cf. [2, form. (22)]), using in addition the bound on the number l of $x_{\kappa_i^*}$ -vertices of D (this bound is contained in the regularity assumption (9)), we estimate in the same way the contribution of the values in κ_i^* into $|\nabla_D w^{\overline{\mathfrak{T}}} - \nabla_D(\mathbb{P}^{\overline{\mathfrak{T}}}\varphi)|$.

(iii) We refer to Section 2.1 and [2, Fig. 2,4] for the notation used in the proof.

First, using the Green-Gauss formula, we can rewrite the value $(\text{div } \vec{\mathcal{F}})_K$ of the discrete function $\mathbb{P}^{\overline{\mathfrak{T}}}(\text{div } \vec{\mathcal{F}})$ in K under the form reminiscent of the form (4) of the discrete divergence operator:

$$(\text{div } \vec{\mathcal{F}})_K = \sum_{s \sim K} \int_{\sigma_s} \vec{\mathcal{F}} \cdot (-1)^{\epsilon_s^K} \vec{n}_s = \sum_{s \sim K} m_s \vec{\mathcal{F}}_{\sigma_s} \cdot (-1)^{\epsilon_s^K} \vec{n}_s.$$

Here $\vec{\mathcal{F}}_{\sigma_s}$ is the mean value of the field $\vec{\mathcal{F}}$ on the part $\sigma_s \subset s$ of the primal interface defining the subdiamond s . One represents analogously the value $(\text{div } \vec{\mathcal{F}})_{K^*}$ of $\mathbb{P}^{\overline{\mathfrak{T}}}(\text{div } \vec{\mathcal{F}})$ in K^* , using the mean values $\vec{\mathcal{F}}_{\sigma_{s_\circ}^*}, \vec{\mathcal{F}}_{\sigma_{s_\oplus}^*}$ of $\vec{\mathcal{F}}$ on the parts $\sigma_{s_\circ}^*, \sigma_{s_\oplus}^* \subset s$ of the dual interface defining s . Recall that s is contained in (or associated with, see [2, Sec. 4]) a diamond D ; it is convenient to define $\vec{\mathcal{F}}_s := \vec{\mathcal{F}}_D$ for all subdiamond s of D . In turn, $\vec{\mathcal{F}}_D$ denotes the value in D of the discrete field $\mathbb{P}^{\overline{\mathfrak{T}}}\vec{\mathcal{F}}$; recall that this is the mean value of the field $\vec{\mathcal{F}}$ on the diamond D .

With this notation in hand, using the definition (2) of the scalar product $\llbracket \cdot, \cdot \rrbracket_\Omega$ and the summation-by parts procedure (recall that $w^{\overline{\mathfrak{T}}}$ is zero on the boundary volumes), analogously to the proof of [2, Prop. 3.2] we get

$$\begin{aligned} & \llbracket \mathbb{P}^{\overline{\mathfrak{T}}}(\text{div } \vec{\mathcal{F}}) - \text{div}^{\overline{\mathfrak{T}}}(\mathbb{P}^{\overline{\mathfrak{T}}}\vec{\mathcal{F}}), w^{\overline{\mathfrak{T}}} \rrbracket_\Omega \\ &= \frac{1}{3} \sum_{s \in \mathfrak{S}} \left((m_s d_{\circ, \oplus}) \frac{w_{\oplus} - w_{\circ}}{d_{\circ, \oplus}} \vec{n}_{\circ, \oplus} \cdot (\vec{\mathcal{F}}_{\sigma_s} - \vec{\mathcal{F}}_s) \right. \\ & \quad \left. + 2 \frac{(w_{i+1}^* - w_i^*)}{d_{i, i+1}^*} \left\{ (m_{s_\circ}^* d_{i, i+1}^*) \vec{n}_{s_\circ}^* \cdot (\vec{\mathcal{F}}_{\sigma_{s_\circ}^*} - \vec{\mathcal{F}}_s) + (m_{s_\oplus}^* d_{i, i+1}^*) \vec{n}_{s_\oplus}^* \cdot (\vec{\mathcal{F}}_{\sigma_{s_\oplus}^*} - \vec{\mathcal{F}}_s) \right\} \right). \end{aligned}$$

Here the summation runs over all subdiamonds $s \in \mathfrak{S}$ represented as $s = S_{\kappa_i^* \kappa_{i+1}^*}^{K_\circ | K_\oplus}$.

Now, notice that the mesh inclination bound (8) implies that for a subdiamond $s = S_{\kappa_i^* \kappa_{i+1}^*}^{K_\circ | K_\oplus}$,

$$(12) \quad \text{reg}(\mathfrak{T}) \text{Vol}(S_{\kappa_i^* \kappa_{i+1}^*}^{K_\circ | K_\oplus}) \geq m_s d_{\circ, \oplus}, \quad \text{reg}(\mathfrak{T}) \text{Vol}(S_{\kappa_i^* \kappa_{i+1}^*}^{K_\circ | K_\oplus}) \geq m_{s_\circ}^* d_{i, i+1}^* + m_{s_\oplus}^* d_{i, i+1}^*,$$

for the case of the meshes described in [2, Sec. 2]. Remark that, if one allows for subdiamonds of negative volume as in [2, Sec. 2], then (12) may loose sense; yet exploiting the restriction on the

number of vertices of $\kappa|L$, one can replace the bound (12) used in the below calculation by the bound

$$\text{reg}(\mathfrak{T}) \text{Vol}(D^{K_\circ|K_\oplus}) \geq m_s d_{\circ,\oplus}, \quad \text{reg}(\mathfrak{T}) \text{Vol}(D^{K_\circ|K_\oplus}) \geq m_{s_\circ}^* d_{i,i+1}^* + m_{s_\oplus}^* d_{i,i+1}^*,$$

which is always true.

From the Lipschitz continuity of $\vec{\mathcal{F}}$, it is clear that

$$|\vec{\mathcal{F}}_{\sigma_s} - \vec{\mathcal{F}}_s|, |\vec{\mathcal{F}}_{\sigma_{s_\circ}^*} - \vec{\mathcal{F}}_s|, |\vec{\mathcal{F}}_{\sigma_{s_\oplus}^*} - \vec{\mathcal{F}}_s| \leq C(\vec{\mathcal{F}}) \text{size}(\mathfrak{T});$$

hence using (12), we get the estimate

$$(13) \quad \left| \left[\mathbb{P}^\mathfrak{T}(\text{div } \vec{\mathcal{F}}) - \text{div}^\mathfrak{T}(\vec{\mathbb{P}}^\mathfrak{T} \vec{\mathcal{F}}), w^\mathfrak{T} \right]_\Omega \right| \leq C(\vec{\mathcal{F}}, \text{reg}(\mathfrak{T})) \text{size}(\mathfrak{T}) \sum_{S \in \mathfrak{S}} \text{Vol}(S) \left(\frac{|w_\oplus - w_\circ|}{d_{\circ,\oplus}} + \frac{|w_{i+1}^* - w_i^*|}{d_{i,i+1}^*} \right).$$

It remains to notice that if $\nabla_s w^\mathfrak{T} = \nabla_D w^\mathfrak{T}$ denotes the value in $s \sim D$ (which means $s \subset D$, for the meshes of [2, Sec. 2]) of the discrete gradient $\nabla^\mathfrak{T} w^\mathfrak{T}$, then

$$\frac{|w_\oplus - w_\circ|}{d_{\circ,\oplus}} = |\text{Proj}_D(\nabla_D w^\mathfrak{T})| \leq |\nabla_D w^\mathfrak{T}|.$$

In addition, because the dual interface $\kappa_\circ|K_\oplus$ is assumed to be a triangle, according to [2, Rem. 5.4] each divided difference $\frac{|w_{i+1}^* - w_i^*|}{d_{i,i+1}^*}$ is precisely the projection of the $2D$ vector $\text{Proj}_D^*(\nabla_D w^\mathfrak{T})$ on the direction of $\overrightarrow{x_{i+1}^* x_i^*}$. Therefore we also have

$$\frac{|w_{i+1}^* - w_i^*|}{d_{i,i+1}^*} \leq |\text{Proj}_D^*(\nabla_D w^\mathfrak{T})| \leq |\nabla_D w^\mathfrak{T}|.$$

Combining (13) with the two latter estimates, we deduce

$$\begin{aligned} \left| \left[\mathbb{P}^\mathfrak{T}(\text{div } \vec{\mathcal{F}}) - \text{div}^\mathfrak{T}(\vec{\mathbb{P}}^\mathfrak{T} \vec{\mathcal{F}}), w^\mathfrak{T} \right]_\Omega \right| &\leq C(\vec{\mathcal{F}}, \text{reg}(\mathfrak{T})) \text{size}(\mathfrak{T}) \sum_{S \in \mathfrak{S}} \text{Vol}(S) |\nabla_s w^\mathfrak{T}| \\ &= C(\vec{\mathcal{F}}, \text{reg}(\mathfrak{T})) \text{size}(\mathfrak{T}) \sum_{D \in \mathfrak{D}} \text{Vol}(D) |\nabla_D w^\mathfrak{T}| = C(\vec{\mathcal{F}}, \text{reg}(\mathfrak{T})) \text{size}(\mathfrak{T}) \|\nabla^\mathfrak{T} w^\mathfrak{T}\|_{L^1(\Omega)}. \end{aligned}$$

(iii-bis) Let $\vec{\mathcal{F}}_D, \vec{\mathcal{F}}_{\kappa|L}$ and $\vec{\mathcal{F}}_{K^*|L^*}$ denote the mean values of $\vec{\mathcal{F}}$ on $D = D_{K^*|L^*}^{K|L}$, on $\kappa|L$ and on $K^*|L^*$, respectively. The claim stems from the fact that on a uniform cartesian mesh, the differences $\vec{\mathcal{F}}_D - \vec{\mathcal{F}}_{\kappa|L}$, $\vec{\mathcal{F}}_D - \vec{\mathcal{F}}_{K^*|L^*}$ are upper bounded by $C(\vec{\mathcal{F}})(\text{size}(\mathfrak{T}))^2$. This follows from the cancellation of the order one terms in the Taylor expansion of $\vec{\mathcal{F}}$ (e.g., we expand $\vec{\mathcal{F}}$ at each point of $\kappa|L$ and use the expansion to calculate the mean value $\vec{\mathcal{F}}_D$ on the diamond $D = D_{K^*|L^*}^{K|L}$ which is symmetrical with respect to $\kappa|L$).

Indeed, for all primal volume K , denote by $\sigma_E(K), \sigma_W(K), \sigma_N(K), \sigma_S(K), \sigma_{\text{abv}}(K), \sigma_{\text{blw}}(K)$ the six interfaces surrounding K (we mimic the notation used in Section 2.2 for the six diamonds surrounding K). Using the definitions of $\vec{\mathbb{P}}^\mathfrak{T}, \text{div}^\mathfrak{T}$ and the Green-Gauss theorem, as in the proof of (iii) we can write

$$\mathbb{P}^\mathfrak{T}(\text{div } \vec{\mathcal{F}}) - \text{div}^\mathfrak{T}(\vec{\mathbb{P}}^\mathfrak{T} \vec{\mathcal{F}}) = \frac{1}{1/N^3} \left\{ \frac{1}{N^2} (\vec{\mathcal{F}}_{\sigma_E(K)} - \vec{\mathcal{F}}_{D_E(K)}) \cdot \vec{i} + \dots + \frac{1}{N^2} (\vec{\mathcal{F}}_{\sigma_{\text{blw}}(K)} - \vec{\mathcal{F}}_{D_{\text{blw}}(K)}) \cdot (-\vec{k}) \right\}.$$

Thus the claim of (iii-bis) is direct from the above bound of order $(\text{size}(\mathfrak{T}))^2 = \frac{1}{N^2}$ on the differences $\vec{\mathcal{F}}_{D_E(K)} - \vec{\mathcal{F}}_{\sigma_E(K)}, \dots, \vec{\mathcal{F}}_{D_{\text{blw}}(K)} - \vec{\mathcal{F}}_{\sigma_{\text{blw}}(K)}$. \square

3.3. Discrete Poincaré inequality, Sobolev embeddings and strong compactness.

The key fact here is the following remark:

Assuming that each face $\kappa\mathcal{L}$ of the mesh \mathfrak{M}° is a triangle, one gets the same embedding results on the 3D CeVe-DDFV meshes as the results known for the two-point discrete gradients on \mathfrak{M}° and on \mathfrak{M}^* .

Indeed, it has been already observed in the proof of Proposition 3.1(iii) that the restriction $l = 3$ on the number l of dual vertices of a diamond $D^{\kappa\circ\kappa\oplus}$ allows for a control by $|\nabla_D w^\overline{\mathfrak{T}}|$ of the divided differences:

$$(14) \quad \frac{|w_\oplus - w_\circ|}{d_{\circ,\oplus}} \leq |\nabla_D w^\overline{\mathfrak{T}}|, \quad \frac{|w_{i+1}^* - w_i^*|}{d_{i,i+1}^*} \leq |\nabla_D w^\overline{\mathfrak{T}}|$$

(here $i = 1, 2, 3$ and by our convention, $w_4^* := w_1^*$, $d_{3,4} := d_{1,3}$; see Fig. 1). Therefore for a proof of the different embeddings, we can treat the primal and the dual meshes in \mathfrak{T} separately, as if our scheme was a scheme with the two-point gradient reconstruction.

If the number l of vertices of a face of \mathfrak{M}° is unrestricted, it is not difficult to construct examples of non-zero discrete functions on Ω , null on $\partial\Omega$, and with non-zero discrete gradient. This phenomenon does not occur if $l \leq 4$; and we justify in Proposition 3.7 the Sobolev embeddings for the uniform rectangular DDFV meshes of Section 2.2. Yet Remark 3.8 below shows that a control on the discrete gradient still allows for oscillations in discrete solutions. The compactness of sub-critical embeddings is false when the primal meshes with quadrangular faces are considered, unless the solution on the dual mesh \mathfrak{M}^* is further separated into two components (which corresponds to a 3D CeVe-DDFV scheme in the spirit of [19]).

Let us first give discrete DDFV versions of the embeddings of the discrete $W_0^{1,p}(\Omega)$ spaces. We mean the embedding into $L^p(\Omega)$ (the Poincaré inequality), into $L^{p^*}(\Omega)$ with $p^* := \frac{3p}{3-p}$, $p < 3$ (the critical Sobolev embedding), as well as the compact embeddings into $L^q(\Omega)$ for all $q < p^*$.

Proposition 3.4.

(i) Let \mathfrak{T} be a 3D CeVe-DDFV mesh of Ω as described in [2, Sec. 2,4]. Let $\text{reg}(\mathfrak{T})$ measure the mesh regularity in the sense (8) and (10). Assume that all primal interface $\kappa\mathcal{L}$ is a triangle.

Let $w^\overline{\mathfrak{T}} \in \mathbb{R}_0^\overline{\mathfrak{T}}$. Then for all $p \in [1, +\infty)$,

$$\|w^{\mathfrak{M}^\circ}\|_{L^p(\Omega)}, \|w^{\mathfrak{M}^*}\|_{L^p(\Omega)} \leq C(p, \Omega, \text{reg}(\mathfrak{T})) \|\nabla^\mathfrak{T} w^\overline{\mathfrak{T}}\|_{L^p(\Omega)}.$$

Moreover, if $p \in [1, 3)$ and $p^* := \frac{3p}{3-p}$, then

$$\|w^{\mathfrak{M}^\circ}\|_{L^{p^*}(\Omega)}, \|w^{\mathfrak{M}^*}\|_{L^{p^*}(\Omega)} \leq C(p, \Omega, \text{reg}(\mathfrak{T})) \|\nabla^\mathfrak{T} w^\overline{\mathfrak{T}}\|_{L^p(\Omega)}.$$

(ii) Let $w^{\overline{\mathfrak{T}}_h} \in \mathbb{R}_0^{\overline{\mathfrak{T}}_h}$ be discrete functions on a family $(\mathfrak{T}_h)_h$ of 3D CeVe-DDFV meshes of Ω as described in [2, Sec. 2,4], parametrized by $h \geq \text{size}(\mathfrak{T}_h)$. Assume that all primal interface $\kappa\mathcal{L}$ is a triangle. Assume that $\sup_{h \in (0, h_{\max})} \text{reg}(\mathfrak{T}_h) < +\infty$, where $\text{reg}(\mathfrak{T}_h)$ measures the regularity of \mathfrak{T}_h in the sense (8) and (10).

Assume that the family $(\nabla^\mathfrak{T}_h w^{\overline{\mathfrak{T}}_h})_{h \in (0, h_{\max})}$ is bounded in $L^p(\Omega)$ for some $p < +\infty$.

Then for all sequence $(h_i)_i$ converging to zero, each of the families $(w^{\mathfrak{M}^\circ h_i})_i$, $(w^{\mathfrak{M}^* h_i})_i$ is relatively compact in $L^q(\Omega)$ for all $q < +\infty$ (if $p \geq 3$) or $q < p^*$ (if $1 \leq p < 3$).

Notice that for the Poincaré inequality (the first statement of (i)), the assumption (10) is not needed: we refer to [11] for a proof of this fact. Actually, with the hint of [11, Lemma 2.6] the Sobolev embeddings for $q \leq p \times 1^* = \frac{3p}{2}$ can be obtained without using (10).

The statements (i),(ii) follow in a very direct way from the proofs given in [28, 17, 29]. Because of (14), the assumption that the primal mesh faces are triangles (i.e., $l = 3$) is a key assumption for the proof. In some of the proofs we refer to, admissibility assumptions on the mesh (such as the mesh orthogonality and assumptions of the kind “ $|x_K - x_L| \leq \text{reg}(\mathfrak{T})|x_K - x_{\kappa\mathcal{L}}|$ ”, see [28, 29])

were imposed. Yet, as in [10] (where the proof of the Poincaré inequality is given for the 2D case), these assumptions are easily replaced with the bounds

$$(15) \quad \begin{aligned} m_{KL} d_{KL} &\leq C(\text{reg}(\mathfrak{T})) \min\{Vol(D^{KL}), Vol(K), Vol(L)\}, \\ m_{K^*|L^*} d_{K^*L^*} &\leq C(\text{reg}(\mathfrak{T})) \min\{Vol(S_{K^*L^*}^{KL}), Vol(K^*), Vol(L^*)\} \end{aligned}$$

that stem from the mesh regularity assumptions (10) and (8).

Remark 3.5. The corresponding embeddings of the discrete space $W^{1,p}(\Omega)$ contain an additional term in the right-hand side, which is usually taken to be either the mean value of $w^{\bar{x}}$ on some fixed part Γ of the boundary $\partial\Omega$ (used when a non-homogeneous Dirichlet boundary condition on Γ is imposed), or the mean value of $w^{\bar{x}}$ on some subdomain ω of Ω (the simplest choice is $\omega = \Omega$, used for the pure Neumann boundary conditions). Let us point out that the strategy of Eymard, Gallouët and Herbin in [29] actually allows to obtain Sobolev embeddings for the “Neumann case” as soon as the Poincaré inequality is obtained. For the proof, one bootstraps the estimate of $\int_{\Omega} |u|^{\alpha}$. First obtained from the Poincaré inequality with $\alpha = p$, it is extended to $\alpha = p \times 1^*$ with the discrete variant [29, Lemma 5.2] (where one can exploit (15)) of the Nirenberg technique. In the same way, the bound of $\int_{\Omega} |u|^{\alpha}$ is further extended to $\alpha = p(1^*)^2$ and so on, until one reaches the critical exponent p^* . The details are given in [6]. Moreover, the Poincaré inequality for the “Neumann case” and $p = 2$ (i.e., the embedding into $L^2(\Omega)$ of the discrete space $\{u \in H^1(\Omega) \mid \int_{\Omega} u = 0\}$) was shown in [29], [35]. The assumption that $p = 2$ is not essential in these proofs, and thus we can consider that the analogue of Proposition 3.4 with the additional terms $|\frac{1}{Vol(\Omega)} \int_{\Omega} w^{\mathfrak{m}^{\circ}}|, |\frac{1}{Vol(\Omega)} \int_{\Omega} w^{\mathfrak{m}^*}|$ in the right-hand side of the estimates is justified.

Remark 3.6. Notice that the same arguments that yield the Poincaré inequality with zero boundary condition yield the trace inequalities of the kind

$$\|w^{\overline{\mathfrak{m}^{\circ}}}\|_{L^p(\Gamma)} \leq C(\Gamma, \Omega, \text{reg}(\mathfrak{T}), p) \left(\|w^{\mathfrak{m}^{\circ}}\|_{L^p(\Omega)} + \|\nabla^{\bar{x}} w^{\bar{x}}\|_{L^p(\Omega)} \right)$$

(the inequality on the dual mesh is completely analogous). These inequalities are useful for treating non-homogeneous Neumann boundary conditions on a part Γ of $\partial\Omega$ (see e.g. [5]).

Now we treat the case of uniform cartesian DDFV meshes.

Proposition 3.7. *Let Ω be the unit cubic domain, $N \in \mathbb{N}$ and let \mathfrak{T} be the mesh of Ω as described in Section 2.2. Then the two claims of Proposition 3.4(i) (as well as the corresponding “Neumann-case” embedding inequalities with the additional term $|\frac{1}{Vol(\Omega)} \int_{\Omega} w^{\bar{x}}|$ in the right-hand side) still hold true.*

PROOF : For a proof, notice that (14) is false for the cubic meshes: more precisely, we see from (6) that $\nabla_D w^{\bar{x}}$ controls the divided differences $|\frac{w_K - w_L}{1/N}|$ of the values of $w^{\bar{x}}$ in all neighbour primal volumes K, L , and also the divided differences $|\frac{w_{K^*} - w_{L^*}}{\sqrt{2}/N}|$ along the diagonals of the faces of primal volumes. Therefore, firstly, the arguments that justify Proposition 3.4(i) also yield the embedding estimates for $w^{\mathfrak{m}^{\circ}}$. Secondly, we replace the dual mesh $\overline{\mathfrak{M}^*}$ by two meshes $\overline{\mathfrak{M}_e^*}, \overline{\mathfrak{M}_o^*}$ such that the edges of each mesh are either the diagonals of the faces of primal volumes, or parts of $\partial\Omega$. Then the same arguments apply to each of the two meshes. To be specific, the family $\overline{\mathfrak{M}^*}$ of the dual volumes (their centers $(x_{K^*})_{K^* \in \overline{\mathfrak{M}^*}}$ form a uniform cartesian net of $\Omega = [0, 1]^3$) is split into two families $\mathfrak{e}^*, \mathfrak{o}^*$. Namely, if a vertex x_{K^*} has the coordinates $(\frac{n_x}{N}, \frac{n_y}{N}, \frac{n_z}{N})$ in the canonic coordinates of \mathbb{R}^3 , then the corresponding volume K^* belongs to the family \mathfrak{e}^* whenever $n_x + n_y + n_z$ is even, and it belongs to the family \mathfrak{o}^* otherwise. Inside Ω , one can connect the dual vertices $(x_{K^*})_{K^* \in \mathfrak{e}^*}$ into a uniform tetrahedral graph of edge length $\sqrt{2}/N$; the same is true for $(x_{K^*})_{K^* \in \mathfrak{o}^*}$. Now, the meshes $\overline{\mathfrak{M}_e^*}$ and $\overline{\mathfrak{M}_o^*}$ are defined as the Voronoï meshes of Ω corresponding to the two separate families $(x_{K^*})_{K^* \in \mathfrak{e}^*}, (x_{K^*})_{K^* \in \mathfrak{o}^*}$ of dual vertices. The Voronoï volumes corresponding to x_{K^*} are denoted by $\widehat{K^*}$ (thus the union for $K^* \in \mathfrak{e}^* \cup \mathfrak{o}^*$ of all Voronoï volumes $\widehat{K^*}$ covers Ω twice). If we define

$$w^{\mathfrak{m}_e^*} := \sum_{K^* \in \mathfrak{e}^*} w_K \mathbb{1}_{\widehat{K^*}}, \quad w^{\mathfrak{m}_o^*} := \sum_{K^* \in \mathfrak{o}^*} w_K \mathbb{1}_{\widehat{K^*}},$$

then the embedding estimates of Proposition 3.4(i) are valid for $w^{\mathfrak{m}_c^*}$ and for $w^{\mathfrak{m}_d^*}$. By construction, $w^{\mathfrak{m}^*}$ takes alternatively the values of $w^{\mathfrak{m}_c^*}$ and $w^{\mathfrak{m}_d^*}$; more precisely,

$$(16) \quad w^{\mathfrak{m}^*} = w^{\mathfrak{m}_c^*} \left(\sum_{K^* \in \mathfrak{e}^*} \mathbb{1}_{K^*} \right) + w^{\mathfrak{m}_d^*} \left(\sum_{K^* \in \mathfrak{o}^*} \mathbb{1}_{K^*} \right).$$

Thus $|w^{\mathfrak{m}^*}| \leq \max\{w^{\mathfrak{m}_c^*}, w^{\mathfrak{m}_d^*}\}$, and we get the desired estimates for $|w^{\mathfrak{m}^*}|$. \square

Remark 3.8. In the situation of Proposition 3.7, the compactness claim from Proposition 3.4(ii) gets wrong. More precisely, the compactness of the families $(w^{\mathfrak{m}^*h})_h$, $(w^{\mathfrak{m}_c^*h})_h$, $(w^{\mathfrak{m}_d^*h})_h$ is true, with the same arguments borrowed from [17, 28, 29]. Yet in general, there is no relation between the accumulation points of the three families. Therefore one can see from formula (16) that the family $(w^{\mathfrak{m}^*h})_h$ may present oscillations.

Let us illustrate the remark with an example. Take a smooth function $w \in \mathcal{D}(\Omega)$, non identically zero, and set

$$\forall K \in \mathfrak{M}^o \quad w_K := 0; \quad \forall x_{K^*} \in \mathfrak{e}^* \quad w_{K^*} := 0; \quad \forall x_{K^*} \in \mathfrak{o}^* \quad w_{K^*} := w(x_{K^*}).$$

In view of (6), and in particular because the discrete gradient $\nabla^\mathfrak{x}$ does not couple the two families \mathfrak{e}^* , \mathfrak{o}^* of dual vertices, the discrete gradient $\nabla^\mathfrak{x} w^{\mathfrak{m}^*}$ is bounded pointwise by $\|\nabla w\|_{L^\infty(\Omega)}$. Yet the family $w^{\mathfrak{m}^*}$ oscillates. Indeed, while $w^{\mathfrak{m}_c^*}$ is identically zero, $w^{\mathfrak{m}_d^*}$ converges in $L^\infty(\Omega)$, as $\text{size}(\mathfrak{T})$ goes to 0, to the non-zero function w . It is easy to see from (16) that $w^{\mathfrak{m}^*}$ converges weakly in $L^q(\Omega)$, $q < +\infty$, to the same limit as $\frac{1}{2}(w^{\mathfrak{m}_c^*} + w^{\mathfrak{m}_d^*})$; and the latter function converges strongly to $\frac{1}{2}(0 + w) = \frac{w}{2}$. The family of the differences $(w^{\mathfrak{m}^*} - \frac{w}{2})$ weakly converges to zero; yet from (16), it oscillates, roughly speaking, between $-\frac{w}{2}$ and $+\frac{w}{2}$. Thus in the above example, the family of $w^{\mathfrak{m}^*}$ it is not compact in the strong $L^q(\Omega)$ topologies.

3.4. Discrete $W^{1,p}(\Omega)$ weak compactness. In relation with Proposition 3.4(ii), let us stress that there is no reason that the components $w^{\mathfrak{m}^o_h}$, $w^{\mathfrak{m}^*h}$ of a sequence $(w^{\mathfrak{x}h})_h$ of discrete functions with bounded in L^p discrete gradients converge to the same limit. Counterexamples are constructed in the same way as in Remark 3.8 above, starting from two distinct smooth functions discretized, one on the primal mesh \mathfrak{M}^o , the other on the dual mesh \mathfrak{M}^* . To cope with this difficulty, the penalization technique of Appendix B can be useful.

The below result shows that in our 3D CeVe-DDFV framework, one should consider that

the “true limit” of discrete functions $w^{\mathfrak{x}h} = (w^{\mathfrak{m}^o_h}, w^{\mathfrak{m}^*h})$ is the limit of $\frac{1}{3}w^{\mathfrak{m}^o_h} + \frac{2}{3}w^{\mathfrak{m}^*h}$.

Proposition 3.9.

(i) Let $w^{\mathfrak{x}h} \in \mathbb{R}_0^{\mathfrak{x}h}$ be discrete functions on a family $(\mathfrak{T}_h)_h$ of 3D CeVe-DDFV meshes of Ω as described in [2, Sec. 2.4], parametrized by $h \geq \text{size}(\mathfrak{T}_h)$. Let us assimilate $w^{\mathfrak{x}h}$ to the piecewise constant functions

$$(17) \quad w^{\mathfrak{x}h}(x) := \frac{1}{3}w^{\mathfrak{m}^o_h} + \frac{2}{3}w^{\mathfrak{m}^*h} = \frac{1}{3} \sum_{K \in \mathfrak{m}^o_h} w_K \mathbb{1}_K(x) + \frac{2}{3} \sum_{K^* \in \mathfrak{m}^*h} w_{K^*} \mathbb{1}_{K^*}(x).$$

Assume that all primal interface $K|L$ is a triangle. Assume that $\sup_{h \in (0, h_{\max}]} \text{reg}(\mathfrak{T}_h) < +\infty$, where $\text{reg}(\mathfrak{T}_h)$ measures the regularity of \mathfrak{T}_h in the sense (7), (8), (9) and (10). Assume that the family $(\nabla^{\mathfrak{x}h} w^{\mathfrak{x}h})_{h \in (0, h_{\max}]}$ is bounded in $L^p(\Omega)$ for some $p \in (1, +\infty)$.

Then for all sequence $(h_i)_i$ converging to zero there exists $w \in W_0^{1,p}(\Omega)$ such that, along a subsequence,

$$(18) \quad \left| \begin{array}{l} w^{\mathfrak{x}h_i} \text{ converges to } w = \frac{1}{3}w^o + \frac{2}{3}w^* \text{ weakly in } L^q(\Omega), \quad q \leq p^* \\ \text{(the components } w^{\mathfrak{m}^o_h}, w^{\mathfrak{m}^*h} \text{ converge to } w^o, w^*, \text{ resp., strongly in } L^q(\Omega), \quad q < p^*) \\ \text{and } \nabla^{\mathfrak{x}h_i} w^{\mathfrak{x}h_i} \text{ converges to } \nabla w \text{ weakly in } L^p(\Omega). \end{array} \right.$$

(ii) If $w^{\mathfrak{x}h} \in \mathbb{R}_0^{\mathfrak{x}h}$ are not assumed to be zero in the boundary volumes, and if the additional assumption of uniform boundedness of

$$m_{w^{\mathfrak{m}^o_h}} := \frac{1}{\text{Vol}(\Omega)} \int_{\Omega} w^{\mathfrak{m}^o_h}, \quad m_{w^{\mathfrak{m}^*h}} := \frac{1}{\text{Vol}(\Omega)} \int_{\Omega} w^{\mathfrak{m}^*h}$$

is imposed, then (18) holds with $w \in W^{1,p}(\Omega)$.

(iii) For the uniform cartesian meshes of Section 2.2, the statement analogous to (i) holds with

$$(19) \quad w^{\mathfrak{x}_h}(x) := \frac{1}{3}w^{\mathfrak{m}^{\circ_h}} + \frac{1}{3}w^{\mathfrak{m}^{\mathfrak{c}_h}} + \frac{1}{3}w^{\mathfrak{m}^{\mathfrak{o}_h^*}} \\ = \frac{1}{3} \sum_{K \in \mathfrak{m}^{\circ_h}} w_K \mathbb{1}_K(x) + \frac{1}{3} \sum_{K^* \in \mathfrak{c}_h^*} w_{K^*} \mathbb{1}_{\widehat{K^*}}(x) + \frac{1}{3} \sum_{K^* \in \mathfrak{o}_h^*} w_{K^*} \mathbb{1}_{\widehat{K^*}}(x);$$

the strong convergence concerns each of the components $w^{\mathfrak{m}^{\circ_h}}$, $w^{\mathfrak{m}^{\mathfrak{c}_h}}$, $w^{\mathfrak{m}^{\mathfrak{o}_h^*}}$.

The statement analogous to (ii) holds if uniform bounds on the mean values of $w^{\mathfrak{m}^{\circ_h}}$ and of $w^{\mathfrak{m}^{\mathfrak{c}_h}}$, $w^{\mathfrak{m}^{\mathfrak{o}_h^*}}$ on Ω are imposed.

It should be noticed that formula (19) is analogous to the natural reconstruction formula for the 3D CeVEFE-DDFV schemes as considered by Coudière and Hubert in [18] and by Eymard, Herbin and Guichard [32].

Remark 3.10.

(i) In the case $p = 1$, the claim remains true with the limit w that belongs to $BV(\Omega) \cap L^{1^*}(\Omega)$, and with discrete gradients converging weakly-* in BV to ∇w .

(ii) The compactness claim for sequences of discrete functions with non-homogeneous boundary conditions on a part of the boundary can be obtained as in [10, Lemma 3.8].

PROOF OF PROPOSITION 3.9:

Let us prove (i). The strong compactness claim for $(w^{\mathfrak{m}^{\circ_h}})_h$ and $(w^{\mathfrak{m}^{\mathfrak{o}_h^*}})_h$ follows by Proposition 3.4(ii); the weak L^{p^*} compactness of $(w^{\mathfrak{x}_h})_h$ comes from Proposition 3.4(i). The weak L^p compactness of the family $(\nabla^{\mathfrak{x}_h} w^{\overline{\mathfrak{x}_h}})_h$ is immediate from its $L^p(\Omega)$ boundedness. Thus if w is the weak L^p limit of a sequence $w^{\mathfrak{x}_h} = \frac{1}{3}w^{\mathfrak{m}^{\circ_h}} + \frac{2}{3}w^{\mathfrak{m}^{\mathfrak{o}_h^*}}$ as $h \rightarrow 0$ and χ is the weak L^p limit of the associated sequence of discrete gradients $\nabla^{\mathfrak{x}_h} w^{\overline{\mathfrak{x}_h}}$, it only remains to show that $\chi = \nabla w$ in the sense of distributions and that w has zero trace on $\partial\Omega$. These two statements follow from the identity

$$(20) \quad \forall \vec{\mathcal{F}} \in \mathcal{D}(\overline{\Omega})^3 \quad \int_{\Omega} \chi \cdot \vec{\mathcal{F}} + \int_{\Omega} w \operatorname{div} \vec{\mathcal{F}} = 0$$

that we now prove. We exploit the discrete duality (1) and the consistency property of Proposition (3.1)(i),(iii).

Take the projection $\vec{\mathbb{P}}^{\mathfrak{x}_h} \vec{\mathcal{F}} \in (\mathbb{R}^3)^{\mathfrak{a}_h}$, $w^{\overline{\mathfrak{x}_h}} \in \mathbb{R}_0^{\overline{\mathfrak{x}_h}}$ and write the discrete duality formula:

$$(21) \quad \left\{ \left\langle \nabla^{\mathfrak{x}_h} w^{\overline{\mathfrak{x}_h}}, \vec{\mathbb{P}}^{\mathfrak{x}_h} \vec{\mathcal{F}} \right\rangle_{\Omega} \right\} + \left[\left[w^{\mathfrak{x}_h}, \operatorname{div}^{\mathfrak{x}_h} (\vec{\mathbb{P}}^{\mathfrak{x}_h} \vec{\mathcal{F}}) \right] \right]_{\Omega} = 0.$$

According to the definition (3) of $\left\{ \left\langle \cdot, \cdot \right\rangle_{\Omega} \right\}$, the first term in (21) is precisely the integral over Ω of the scalar product of the constant per diamond fields $\nabla^{\mathfrak{x}_h} w^{\overline{\mathfrak{x}_h}}$ and $\vec{\mathbb{P}}^{\mathfrak{x}_h} \vec{\mathcal{F}}$. By Proposition 3.1(i) and the definition of χ , this term converges to the first term in (20) as $h \rightarrow 0$. Similarly, introducing the projection $\mathbb{P}^{\mathfrak{x}_h}(\operatorname{div} \vec{\mathcal{F}})$ of $\operatorname{div} \vec{\mathcal{F}}$ on $\mathbb{R}^{\mathfrak{x}_h}$, from the definition (2) of $\left[\left[\cdot, \cdot \right] \right]_{\Omega}$, Proposition 3.1(i) and the definition of $w^{\overline{\mathfrak{x}_h}}$ in (17) we see that, as $h \rightarrow 0$,

$$\left[\left[w^{\mathfrak{x}_h}, \mathbb{P}^{\mathfrak{x}_h}(\operatorname{div} \vec{\mathcal{F}}) \right] \right]_{\Omega} \longrightarrow \frac{1}{3} \int_{\Omega} (\lim_{h \rightarrow 0} w^{\mathfrak{m}^{\circ_h}}) \operatorname{div} \vec{\mathcal{F}} + \frac{2}{3} \int_{\Omega} (\lim_{h \rightarrow 0} w^{\mathfrak{m}^{\mathfrak{o}_h^*}}) \operatorname{div} \vec{\mathcal{F}} = \int_{\Omega} w \operatorname{div} \vec{\mathcal{F}}.$$

It remains to invoke Proposition (3.1)(iii) and the $L^1(\Omega)$ bound on $\nabla^{\mathfrak{x}_h} w^{\overline{\mathfrak{x}_h}}$ to justify the fact that

$$\lim_{h \rightarrow 0} \left[\left[w^{\mathfrak{x}_h}, \operatorname{div}^{\mathfrak{x}_h} (\vec{\mathbb{P}}^{\mathfrak{x}_h} \vec{\mathcal{F}}) \right] \right]_{\Omega} = \lim_{h \rightarrow 0} \left[\left[w^{\mathfrak{x}_h}, \mathbb{P}^{\mathfrak{x}_h}(\operatorname{div} \vec{\mathcal{F}}) \right] \right]_{\Omega}.$$

For a proof of (ii), one uses the versions of the compact Sobolev embeddings with control by the mean value in Ω , and uses test functions $\vec{\mathcal{F}}$ compactly supported in Ω .

The point (iii) is shown with the same arguments, using Proposition 3.1(iii-bis) and (16). \square

3.5. Discrete operators, functions and fields on $(0, T) \times \Omega$. Whenever evolution equations are discretized in space with the help of the DDFV operators as described above, analogous consistency properties, Poincaré inequality and discrete $L^p(0, T; W^{1,p}(\Omega))$ compactness properties hold.

To be specific, given a CeVe-DDFV mesh \mathfrak{T} of Ω and a time step Δt , one considers the additional projection operator

$$\mathbb{S}^{\Delta t} : f \mapsto (f^n)_{n \in [1, N_{\Delta t}]} \subset L^1(\Omega), \quad f^n(x) := \frac{1}{\Delta t} \int_{(n-1)\Delta t}^{n\Delta t} f(t, x) dt.$$

Here f can mean a function in $L^1((0, T) \times \Omega)$ or a field in $(L^1((0, T) \times \Omega))^3$. The smallest integer greater than or equal to $T/\Delta t$ is denoted by $N_{\Delta t}$. It is always meant that n takes values in $[1, T/\Delta t] \cap \mathbb{N}$; in other words, n takes the values $1, \dots, N_{\Delta t}$.

One defines discrete functions $w^{\mathfrak{T}, \Delta t} \in (\mathbb{R}^{\mathfrak{T}})^{N_{\Delta t}}$ on $(0, T) \times \Omega$ as collections of discrete functions $w^{\mathfrak{T}, n}$ on Ω parametrized by $n \in [1, N_{\Delta t}]$. Discrete functions $w^{\mathfrak{T}, \Delta t} \in (\mathbb{R}^{\overline{\mathfrak{T}}})^{N_{\Delta t}}$ on $(0, T) \times \overline{\Omega}$ and discrete fields $\vec{F}^{\mathfrak{T}, \Delta t} \in ((\mathbb{R}^3)^{\mathfrak{D}})^{N_{\Delta t}}$ are defined similarly.

The associated norms are defined in a natural way; e.g., the discrete $L^p(0, T; W_0^{1,p}(\Omega))$ norm of a discrete function $w^{\mathfrak{T}, n} \in (\mathbb{R}^{\overline{\mathfrak{T}}})^{N_{\Delta t}}$ is computed as

$$\sum_{n=1}^{N_{\Delta t}} \Delta t \|\nabla^{\mathfrak{T}} w^{\mathfrak{T}, n}\|_{L^p(\Omega)}.$$

To treat space-time dependent test functions and fields in the way of Proposition 3.1, one replaces the projection operators $\mathbb{P}^{\mathfrak{T}}$ (and its components $\mathbb{P}^{\mathfrak{m}^o}, \mathbb{P}^{\mathfrak{m}^*}$), $\mathbb{P}^{\overline{\mathfrak{T}}}$ and $\overline{\mathbb{P}}^{\mathfrak{T}}$ by their compositions with $\mathbb{S}^{\Delta t}$. Then the statement and the proof of Proposition 3.1 and Corollary 3.3 are extended in a straightforward way.

Also the statement of Proposition 3.9 extends naturally to this time-dependent case; one only has to replace the statement (18) with the weak $L^p(0, T; W^{1,p}(\Omega))$ convergence statement:

$$(22) \quad \left\{ \begin{array}{l} w^{\mathfrak{T}_h, \Delta t_h} \text{ converges to } w = \frac{1}{3}w^o + \frac{2}{3}w^* \text{ weakly in } L^p((0, T) \times \Omega) \\ \text{(and the components } w^{\mathfrak{m}^o_h}, w^{\mathfrak{m}^*_h} \text{ converge to } w^o, w^*, \text{ resp., weakly in } L^p((0, T) \times \Omega)) \\ \text{and } \nabla^{\mathfrak{T}_h} w^{\mathfrak{T}_h, \Delta t_h} \text{ converges to } \nabla w \text{ weakly in } L^p(\Omega) \end{array} \right.$$

as $\text{size}(\mathfrak{T}_h) + \Delta t_h \rightarrow 0$. It is natural that strong compactness on the space-time cylinder $(0, T) \times \Omega$ not follow from the sole space discrete gradient bound; one also needs some control of time oscillations. It is also well known that this control can be a very weak one (cf. e.g. the well-known Aubin-Lions and Simon lemmas; see [34] for a discrete version). In the next section, we give the discrete version of a similar result due to Kruzhkov [44].

3.6. Strong compactness in $L^1((0, T) \times \Omega)$. Here we state a lemma that combines a basic space translates estimate (for the ‘‘compactness in space’’) with the Kruzhkov L^1 time compactness lemma (see [44]). Actually, the Kruzhkov lemma is, by essence, a local compactness result. For the sake of simplicity, we state and prove the version suitable for discrete functions null on the boundary; the general $L^1_{loc}([0, T] \times \Omega)$ version can be shown with the same arguments (cf. [6]).

Proposition 3.11. *Let $(u^{\mathfrak{T}_h, \Delta t_h})_h \in (\mathbb{R}^{\overline{\mathfrak{T}_h}})^{N_{\Delta t_h}}$ be a family of discrete functions on the cylinder $(0, T) \times \Omega$ corresponding to a family $(\Delta t_h)_h$ of time steps and to a family $(\mathfrak{T}_h)_h$ of 3D CeVe-DDFV meshes of Ω as described in [2, Sec. 2,4]; we mean that $h \geq \text{size}(\mathfrak{T}_h) + \Delta t_h$.*

Assume that $\sup_{h \in (0, h_{max})} \text{reg}(\mathfrak{T}_h) < +\infty$, where $\text{reg}(\mathfrak{T}_h)$ measures the regularity of \mathfrak{T}_h in the sense (7) and (8). Assume that every primal interface $k|L$ for all mesh \mathfrak{T}_h is a triangle.

For all $h > 0$, assume that discrete functions $u^{\mathfrak{T}_h, \Delta t_h}$ satisfy the discrete evolution equations

$$(23) \quad \text{for } n \in [1, N_{\Delta t_h}], \quad \frac{b(u^{\mathfrak{T}_h, n}) - b(u^{\mathfrak{T}_h, n-1})}{\Delta t} = \text{div}^{\mathfrak{T}_h} \vec{F}^{\mathfrak{T}_h, n} + f^{\mathfrak{T}_h, n}$$

with some fixed uniformly continuous³ non-decreasing function $b : \mathbb{R} \rightarrow \mathbb{R}$, with some initial data $b(u^{\mathfrak{T}_h, 0}) \in \mathbb{R}^{\mathfrak{T}_h}$, source terms $f^{\mathfrak{T}_h, \Delta t_h} \in (\mathbb{R}^{\mathfrak{T}_h})^{N_{\Delta t_h}}$ and discrete fields $\vec{F}^{\mathfrak{T}_h, \Delta t_h} \in ((\mathbb{R}^3)^{\mathfrak{D}_h})^{N_{\Delta t_h}}$.

³Mere continuity of $b(\cdot)$ is enough if the families $(b(u^{\mathfrak{m}^o_h, \Delta t_h}))_h$, $(b(u^{\mathfrak{m}^*_h, \Delta t_h}))_h$ are equi-integrable.

Assume that there exists a constant M such that the uniform $L^1((0, T) \times \Omega)$ estimates hold:

$$(24) \quad \sum_{n=1}^{N\Delta t_h} \Delta t \left(\|b(u^{\mathfrak{M}^o_h, n})\|_{L^1(\Omega)} + \|b(u^{\mathfrak{M}^*_h, n})\|_{L^1(\Omega)} \right. \\ \left. + \|f^{\mathfrak{M}^o_h, n}\|_{L^1(\Omega)} + \|f^{\mathfrak{M}^*_h, n}\|_{L^1(\Omega)} + \|\vec{\mathcal{F}}^{\mathfrak{M}^*_h, n}\|_{L^1(\Omega)} \right) \leq M,$$

and, moreover, the uniform $L^1((0, T) \times \Omega)$ estimate on $\nabla^{\mathfrak{M}^*_h} u^{\mathfrak{M}^*_h, \Delta t_h}$ holds:

$$(25) \quad \sum_{n=1}^{N\Delta t_h} \Delta t \|\nabla^{\mathfrak{M}^*_h} u^{\mathfrak{M}^*_h, n}\|_{L^1(\Omega)} \leq M.$$

Assume that the families $(b(u^{\mathfrak{M}^o_h, 0}))_h, (b(u^{\mathfrak{M}^*_h, 0}))_h$ are bounded in $L^1(\Omega)$.

Then for all sequence $(h_i)_i$ converging to zero there exist $\beta^o, \beta^* \in L^1((0, T) \times \Omega)$ such that, along a subsequence,

$$b(u^{\mathfrak{M}^o_{h_i}, \Delta t_{h_i}}) \longrightarrow \beta^o \quad \text{and} \quad b(u^{\mathfrak{M}^*_{h_i}, \Delta t_{h_i}}) \longrightarrow \beta^* \quad \text{in } L^1((0, T) \times \Omega) \text{ as } i \rightarrow \infty.$$

Notice that the specific structure of the DDFV meshes is not important for the above result, neither the dimension; we refer to [6] for a version of the lemma on the admissible finite volume meshes in the sense of [28]. Yet, contrarily to the situation with the Sobolev compact embedding results, in the proof of Proposition 3.11 the two meshes $\mathfrak{M}^o, \mathfrak{M}^*$ should not be considered separately; and the discrete duality (1) is an important ingredient of the proof. We postpone the proof of Proposition 3.11 to Appendix A.

4. APPLICATIONS AND CONVERGENCE PROOFS

Here we describe the application of the DDFV schemes to the discretization of three classes of nonlinear elliptic or degenerate parabolic PDEs. In Sections 4.1 and 4.2, the role of the weak formulation of the scheme (coming from the discrete duality property) in the convergence proofs is emphasized; and the preceding results and hints are combined into sketchy convergence proofs. In Section 4.3, we briefly discuss the additional ‘‘dissipation property’’ that holds for orthogonal DDFV meshes and allows for analysis involving nonlinear test functions of the unknown solution.

The ideas and the hints of Sections 4.1–4.3 are taken from the works [10] (see also [11] and Alt and Luckhaus [1]), [3] and [5]. For details, we refer to the aforementioned papers.

4.1. Leray-Lions elliptic and parabolic problems. Following Alt and Luckhaus [1] (see also [46]), we consider the problem

$$(26) \quad \begin{cases} b(u)_t = \operatorname{div} \varphi(\nabla u) + f \\ u_{(0, T) \times \partial \Omega} = 0, \quad b(u)_{t=0} = b_0, \end{cases}$$

for $b : \mathbb{R} \rightarrow \mathbb{R}$ a continuous non-decreasing function with $b(0) = 0$, and for

$$-\operatorname{div} \varphi(\nabla \cdot) : W_0^{1, p}(\Omega) \rightarrow W^{-1, p'}(\Omega)$$

which is a Leray-Lions operator; namely,

$$(27) \quad \begin{cases} \varphi \in C(\mathbb{R}^3, \mathbb{R}^3), \quad \forall \xi \neq \eta \quad (\varphi(\xi) - \varphi(\eta)) \cdot (\xi - \eta) > 0; \\ \forall \xi \quad \varphi(\xi) \cdot \xi \geq c|\xi|^p, \quad |\varphi(\xi)|^{p'} \leq C(1 + |\xi|^p) \end{cases}$$

with $p \in (1, +\infty)$ and p' the conjugate exponent of p . The p -laplacian operator, i.e., $\varphi(\xi) = |\xi|^{p-2}\xi$, is the main example in the applications; more generally, it can be combined with an anisotropy and heterogeneity, as for the case $\varphi(\xi, x) = |A(x)\xi|^{p-2}A(x)\xi$, $(A(x))_{x \in \Omega}$ being a uniformly elliptic bounded family of symmetric matrices. Due to the non-strict monotonicity of b and the possible degeneracy/singularity of the diffusion coefficient $\varphi'(\nabla u)$, problem (26) is a degenerate parabolic problem (for $b \equiv 0$ and f constant in t , it reduces to an elliptic problem).

We consider $f \in L^{p'}(Q)$ the so-called ‘‘finite energy initial data’’ b_0 , i.e.,

$$b_0 : \Omega \mapsto \operatorname{Range}(b), \quad b_0 = b(u_0) \quad \text{with the restriction} \quad B(u_0) = \int_0^{u_0} s \, db(s) \in L^1(\Omega).$$

Finite volume discretization of (26) in the parabolic case and its convergence were studied in [11]. Different finite volume schemes and their convergence in the elliptic case were studied in

[7, 10, 26, 30]; error estimates were obtained, in three different situations, in [7, 8, 9]; the important refinements for the case with discontinuous coefficients were introduced in [15].

Let us consider the following time-implicit DDFV scheme for (26):

$$(28) \quad \begin{aligned} & \text{find } u^{\mathfrak{x}, \Delta t} = (u^{\mathfrak{x}, n})_{n=1..N_{\Delta t}} \in \mathbb{R}_0^{\overline{\mathfrak{x}}} \text{ such that} \\ & \forall n = 1..N_{\Delta t} \quad \frac{b(u^{\mathfrak{x}, n}) - b(u^{\mathfrak{x}, n-1})}{\Delta t} = \operatorname{div}^{\mathfrak{x}} \varphi(\nabla^{\mathfrak{x}} u^{\overline{\mathfrak{x}, n}}) + f^{\mathfrak{x}, n} + \mathcal{P}^{\mathfrak{x}}[u^{\overline{\mathfrak{x}, n}}] \end{aligned}$$

with the initial conditions and source term given by

$$(29) \quad b(u^{\mathfrak{x}, 0}) = \mathbb{P}^{\mathfrak{x}} b_0, \quad f^{\mathfrak{x}, n} = \mathbb{P}^{\mathfrak{x}} (\mathbb{S}^{\Delta t} f)^n.$$

The notation is the one of Sections 2 and 3.5, except for the penalization operator $\mathcal{P}^{\mathfrak{x}}[\cdot]$ introduced and explained in Appendix B. The penalization term serves for the convergence proof; in practice the numerical scheme without this term converges as well. Penalization can also be replaced by a more intricate approximation of the time evolution term; see Remark 6.3 in Appendix C.

The scheme thus leads to a nonlinear system to be solved at each time step; for a description of the strategy for solving the resulting nonlinear algebraic equations, see [15] and Appendix D.

Proposition 4.1. *A discrete function $u^{\mathfrak{x}, \Delta t}$ solves (28) if and only if there holds the weak formulation:*

$$(30) \quad \begin{aligned} & \forall n = 1..N_{\Delta t} \quad \forall v^{\mathfrak{x}} \in \mathbb{R}_0^{\overline{\mathfrak{x}}} \\ & \left[\left[\frac{b(u^{\mathfrak{x}, n}) - b(u^{\mathfrak{x}, n-1})}{\Delta t}, v^{\mathfrak{x}} \right]_{\Omega} + \left\{ \left\{ \varphi(\nabla^{\mathfrak{x}} u^{\overline{\mathfrak{x}, n}}), \nabla^{\mathfrak{x}} v^{\overline{\mathfrak{x}}} \right\} \right\}_{\Omega} \right. \\ & \quad \left. = \left[\left[f^{\mathfrak{x}, n}, v^{\mathfrak{x}} \right]_{\Omega} + \frac{2}{3} \sum_{K \in \overline{\mathfrak{M}^{\sigma}}, K^* \in \overline{\mathfrak{M}^{\mathfrak{x}}}} \operatorname{Vol}(K \cap K^*) \frac{(u_K^n - u_{K^*}^n)(v_K - v_{K^*})}{\operatorname{size}(\mathfrak{T})} \right. \right. \end{aligned}$$

Formulation (28) with the initial condition implies the following weak space-and-time formulation:

$$(31) \quad \begin{aligned} & - \sum_{n=0}^{N_{\Delta t}-1} \Delta t \left[\left[b(u^{\mathfrak{x}, n}), \frac{v^{\mathfrak{x}, n+1} - v^{\mathfrak{x}, n}}{\Delta t} \right]_{\Omega} + \sum_{n=1}^{N_{\Delta t}} \Delta t \left\{ \left\{ \varphi(\nabla^{\mathfrak{x}} u^{\overline{\mathfrak{x}, n}}), \nabla^{\mathfrak{x}} v^{\overline{\mathfrak{x}, n}} \right\} \right\}_{\Omega} \right. \\ & \quad = \sum_{n=1}^{N_{\Delta t}} \Delta t \left[\left[f^{\mathfrak{x}, n}, v^{\mathfrak{x}, n} \right]_{\Omega} + \left[\left[b(u^{\mathfrak{x}, 0}), v^{\mathfrak{x}, 0} \right]_{\Omega} \right. \right. \\ & \quad \quad \left. \left. + \frac{2}{3} \sum_{n=1}^{N_{\Delta t}} \Delta t \sum_{K \in \overline{\mathfrak{M}^{\sigma}}, K^* \in \overline{\mathfrak{M}^{\mathfrak{x}}}} \operatorname{Vol}(K \cap K^*) \frac{(u_K^n - u_{K^*}^n)(v_K - v_{K^*})}{\operatorname{size}(\mathfrak{T})} \right] \right. \end{aligned}$$

for all test function $v^{\mathfrak{x}, \Delta t}$ such that $v^{\mathfrak{x}, N} = 0$.

For the proof, the deduction of (30), (31) from (28) is straightforward using the discrete duality, Proposition 6.1 and (for getting (31)) using the Abel transformation of the sum in n . Conversely, to get from (30) to (28) one uses the test functions $v^{\mathfrak{x}}$ with only one non-zero entry.

Theorem 4.2. *Assume that b , b_0 and φ satisfy the assumptions of the beginning of this section. Let \mathfrak{T} be a CeVe-DDFV mesh as described in the introduction, further assume that it is either a uniform cartesian mesh, or a mesh such that every primal interface $K|L$ is a triangle. Let $\Delta t > 0$ be a time step. There exists a unique solution to scheme (28), (29).*

Further, assume we are given a family $(\Delta t_h)_h$ of time steps and a family $(\mathfrak{T}_h)_h$ of CeVe-DDFV meshes (with $\Delta t_h + \operatorname{size}(\mathfrak{T}_h) \leq h$) satisfying the uniform regularity assumptions (7), (8), (9) and (10). Let $u^{\mathfrak{x}_h, \Delta t_h}$ denote the corresponding discrete solution, and $\nabla^{\mathfrak{x}} u^{\overline{\mathfrak{x}_h, \Delta t_h}}$ denote the corresponding discrete gradient of the solution (both are considered as functions of Q). Then as $h \rightarrow 0$, there holds

$$b(u^{\mathfrak{x}_h, \Delta t_h}) \rightarrow b(u) \text{ in } L^1(Q), \quad u^{\mathfrak{x}_h, \Delta t_h} \rightarrow u \text{ in } L^p(Q), \quad \text{and} \quad \nabla^{\mathfrak{x}} u^{\overline{\mathfrak{x}_h, \Delta t_h}} \rightarrow \nabla u \text{ in } L^p(Q),$$

where $u \in L^p(0, T; W_0^{1,p}(\Omega))$ is the unique solution of (26).

Now we turn to the proof of Theorem 4.2.

PROOF (SKETCHED): The weak formulations (30),(31) (coming from the discrete duality) are the main tool, along with the “discrete versions” of the arguments of Alt and Luckhaus [1].

The proof is not specific to dimension three, the same result and proof apply for the 2D DDFV schemes (cf. [3] for a unified treatment). Before passing to the limit $h \rightarrow 0$, we drop the subscript h from the notation Δt_h and \mathfrak{T}_h .

Uniqueness of a discrete solution follows from the monotonicity of $b(\cdot)$, $\varphi(\cdot)$. Indeed, by induction in n , we obtain the equality

$$\left[b(u^{\bar{x},n}) - b(\hat{u}^{\bar{x},n}), u^{\bar{x},n} - \hat{u}^{\bar{x},n} \right]_{\Omega} + \Delta t \left\{ \varphi(\nabla^{\bar{x}} u^{\bar{x},n}) - \varphi(\nabla^{\bar{x}} \hat{u}^{\bar{x},n}), \nabla^{\bar{x}} u^{\bar{x},n} - \nabla^{\bar{x}} \hat{u}^{\bar{x},n} \right\}_{\Omega} \leq 0$$

(here $u^{\bar{x},\Delta t}$, $\hat{u}^{\bar{x},\Delta t}$ are two discrete solutions, and we have used (30) at time step n with the test function $v^{\bar{x}} = u^{\bar{x},n} - \hat{u}^{\bar{x},n}$; the inequality “ \leq ” comes from the penalization term which is dropped, because it is non-negative). The strict monotonicity of $\varphi(\cdot)$ implies that $\nabla^{\bar{x}} u^{\bar{x},n} = \nabla^{\bar{x}} \hat{u}^{\bar{x},n}$, whence $u^{\bar{x},n} = \hat{u}^{\bar{x},n}$ from the discrete Poincaré inequality of Proposition 3.4(ii) or Proposition 3.7.

Further, existence of a discrete solution follows by an application of the Brouwer fixed-point theorem or of the finite-dimensional topological degree theory from the *a priori* estimates we now prove (see e.g. [11, 10, 26, 30]). Indeed, first note the following convexity inequality:

$$(32) \quad (b(z) - b(\hat{z}))z \geq B(z) - B(\hat{z}) \quad \text{with} \quad B(z) = \int_0^z s \, db(s).$$

Assume $u^{\bar{x},\Delta t}$ is a solution of (28),(29). Using $v^{\bar{x}} = u^{\bar{x},n}$ as test function in formulation (30) at time step n , summing in n from 1 to k , $k \leq N_{\Delta t}$ and using (32) for the time evolution terms, the coercivity (27) in the diffusion term and the Young and discrete Poincaré inequalities in the source term, we find the *a priori* bound

$$(33) \quad \max_{1 \leq k \leq N_{\Delta t}} \left(\sum_K m_K B(u_K) + \sum_{K^*} m_{K^*} B(u_{K^*}) \right) + \sum_{n=1}^{N_{\Delta t}} \Delta t \sum_D m_D |\nabla_D u^{\bar{x},n}|^p + \sum_{n=1}^{N_{\Delta t}} \Delta t \left[\mathcal{P}^{\bar{x}} u^{\bar{x},n}, u^{\bar{x},n} \right]_{\Omega} \leq \text{const} (\|f\|_{L^{p'}(Q)}^{p'} + \|B(u_0)\|_{L^1(\Omega)}).$$

Notice that in the variational case, i.e., for $\varphi = \nabla \Phi$, the discrete duality allows to show (see e.g. [10]) that the discrete solution $u^{\bar{x},n}$ at time step n is the unique minimizer of the following convex coercive functional:

$$J^n[u^{\bar{x}}] := \frac{1}{3} \sum_K m_K D(u_K) + \frac{2}{3} \sum_{K^*} m_{K^*} D(u_{K^*}) + \Delta t \sum_D m_D \Phi(\nabla_D u^{\bar{x}}) - \left[\Delta t f^{\bar{x},n} + b(u^{\bar{x},n-1}), u^{\bar{x}} \right]_{\Omega} + \frac{1}{3} \sum_{K \in \overline{\mathfrak{M}^{\circ}}, K^* \in \overline{\mathfrak{M}^*}} \text{Vol}(K \cap K^*) \frac{(u_K - u_{K^*})^2}{\text{size}(\mathfrak{T})},$$

where $D(\cdot)$ is a primitive of $b(\cdot)$. This variational point of view may be useful for a practical implementation of the nonlinear scheme using descent algorithms (cf. [7, 10]); the coordination-decomposition approach of [37] is a more general and more efficient alternative, see [15]. We recall this algorithm in Appendix D.

Now, estimate (33) contains, in particular, a uniform $L^p(Q)$ bound on the discrete functions $\nabla^{\bar{x}_h} u^{\bar{x}_h, \Delta t_h}$. Then the compactness result (22) permits to extract a subsequence (here and in the sequel, extracted subsequences are not relabelled) such that

$$\nabla^{\bar{x}_h} u^{\bar{x}_h, \Delta t_h} \rightharpoonup \nabla u \text{ in } L^p(Q) \text{ weakly with } u \in L^p(0, T; W_0^{1,p}(\Omega))$$

$$\text{and } u := \frac{1}{3} u^{\circ} + \frac{2}{3} u^* \text{ with } u^{\circ} \rightharpoonup u^{\circ} \text{ and } u^* \rightharpoonup u^* \text{ in } L^p(Q) \text{ weakly}$$

(the lack of control of time oscillations precludes us from getting the strong convergence here). Moreover, Proposition 6.2 says us that $u^{\circ} = u^* = u$. From the growth assumption in (27) we infer the convergence $\varphi(\nabla^{\bar{x}_h} u^{\bar{x}_h, \Delta t_h}) \rightharpoonup \chi$ weakly in $L^{p'}(Q)$. Furthermore, the $L^1(Q)$ estimate

of $\nabla^{\bar{x}_h} u^{\bar{x}_h, \Delta t_h}$, the discrete evolution equations (28) and the discrete Kruzhkov lemma permit to get the strong convergences

$$b(u^{\mathfrak{m}^o_h, \Delta t_h}) \rightarrow \beta^o \text{ and } b(u^{\mathfrak{m}^*_h, \Delta t_h}) \rightarrow \beta^* \text{ in } L^1(Q)$$

(notice that (33) and the definition of $B(\cdot)$ imply equi-integrability of $b(u^{\mathfrak{m}^o_h, \Delta t_h})$, $b(u^{\mathfrak{m}^*_h, \Delta t_h})$, so that mere continuity of $b(\cdot)$ is enough). The monotonicity of $b(\cdot)$ permits to identify both β^o and β^* with $b(u)$, using the equi-integrability of $(u^{\mathfrak{m}^o_h, \Delta t_h})_h$, $(u^{\mathfrak{m}^*_h, \Delta t_h})_h$ and the Minty argument. Consequently, we also have the strong convergence

$$B(u^{\mathfrak{m}^o_h, \Delta t_h}) \rightarrow B(u) \text{ and } B(u^{\mathfrak{m}^*_h, \Delta t_h}) \rightarrow B(u) \text{ in } L^1(Q).$$

Without loss of restriction, we may assume that the above convergence also takes place in $L^1(\Omega)$ for $t = T$ (this takes place for a.e. $T > 0$). Now, we can pass to the limit in the weak discrete formulation (31) (using, in particular, Corollary 3.3 for the initial condition term, using the parabolic version of Corollary 3.3 for the source term, and using the parabolic analogue of Proposition 3.1 for the test function) to get

$$(34) \quad - \iint_Q b(u)v_t - \int_{\Omega} b_0 v(0, \cdot) + \iint_Q \chi \cdot \nabla v = \iint_Q f v$$

with regular test functions v that are zero at $t = T$. Then, in the way of Alt and Luckhaus [1] we can write (34) under the equivalent ‘‘variational’’ formulation with test functions $v \in X = L^p(0, T; W_0^{1,p}(\Omega))$, using the duality product to give sense to the product of v by $b(u)_t \in X^* = L^{p'}(0, T; W^{-1,p'}(\Omega))$:

$$- \iint_Q b(u)v_t - \int_{\Omega} b_0 v(0, \cdot) \text{ becomes } \int_0^T \langle b(u)_t, v \rangle_{W^{-1,p'}, W_0^{1,p}}.$$

The key step is to identify χ (the weak limit of $\chi^{\bar{x}_h, \Delta t_h} := \varphi(\nabla^{\bar{x}_h} u^{\bar{x}_h, \Delta t_h})$) with $\varphi(\nabla u)$ (see, e.g., [1]). This is done starting from the weak formulation (30), with $v^{\bar{x}_h} = u^{\bar{x}_h, n}$ at the time step n : summing in n from 1 to $N_{\Delta t_h}$ and using the convexity inequality (32), we get

$$\begin{aligned} & \frac{1}{3} \sum_{\kappa} m_{\kappa} B(u_{\kappa}^{N_{\Delta t_h}}) + \frac{2}{3} \sum_{\kappa^*} m_{\kappa^*} B(u_{\kappa^*}^{N_{\Delta t_h}}) + \sum_{n=1}^{N_{\Delta t_h}} \Delta t_h \left\{ \varphi(\nabla^{\bar{x}_h} u^{\bar{x}_h, \Delta t_h}), \nabla^{\bar{x}_h} u^{\bar{x}_h, \Delta t_h} \right\}_{\Omega} \\ & \leq \sum_{n=1}^{N_{\Delta t_h}} \Delta t_h \left[\left[f^{\bar{x}_h, n}, u^{\bar{x}_h, n} \right]_{\Omega} \right] + \frac{1}{3} \sum_{\kappa} m_{\kappa} B(u_{\kappa}^0) + \frac{2}{3} \sum_{\kappa^*} m_{\kappa^*} B(u_{\kappa^*}^0). \end{aligned}$$

Notice that the penalization term can has the good sign and it is dropped in the above inequality. Using Corollary 3.3 and the continuity of $B(z)$ as function of $b(z)$ (for the initial condition term) and using the parabolic version of Corollary 3.3 (for the source term), from the previously obtained weak convergences we deduce

$$(35) \quad \lim_{h \rightarrow 0} \sum_{n=1}^{N_{\Delta t_h}} \Delta t_h \left\{ \varphi(\nabla^{\bar{x}_h} u^{\bar{x}_h, \Delta t_h}), \nabla^{\bar{x}_h} u^{\bar{x}_h, \Delta t_h} \right\}_{\Omega} \geq \iint_Q f u - \int_{\Omega} (B(u(T)) - B(u_0));$$

at this point, we have used that $B(u^o) \equiv B(u^*) \equiv B(u)$. By the integration-by-parts argument of [1, 46],

$$\int_{\Omega} (B(u(T)) - B(u_0)) = \int_0^T \langle b(u)_t, u \rangle_{W^{-1,p'}, W_0^{1,p}}.$$

Thus the right-hand side of (35) can be written as

$$\iint_Q f u - \int_0^T \langle b(u)_t, u \rangle_{W^{-1,p'}, W_0^{1,p}} \quad \text{and then, due to (34), as } \iint_Q \chi \cdot \nabla u.$$

Hence we get the inequality

$$(36) \quad \iint_Q \chi \cdot G \geq \liminf_{h \rightarrow 0} \sum_{n=1}^{N_{\Delta t_h}} \Delta t_h \left\{ \varphi(\nabla^{\bar{x}_h} u^{\bar{x}_h, \Delta t_h}), \nabla^{\bar{x}_h} u^{\bar{x}_h, \Delta t_h} \right\}_{\Omega} = \liminf_{h \rightarrow 0} \varphi(G_h) \cdot G_h,$$

with $G = \nabla u$ and $G_h = \nabla^{\bar{x}_h} u^{\bar{x}_h, \Delta t_h}$. With (36) in hand, the monotonicity of $\varphi(\cdot)$ in (27) and the classical Minty-Browder argument (see e.g. [1]; cf. [10, 26, 30] for its use in finite volumes) ensures that $\chi = \varphi(G)$ and, moreover, the strict monotonicity of $\varphi(\cdot)$ yields strong convergence in $L^p(Q)$ of G_h to G .

With $\chi = \varphi(\nabla u)$, we see that (34) is indeed the weak formulation of problem (26); thus u is a solution of the problem. The uniqueness of a solution permits to get the convergence results as $h \rightarrow 0$ without extracting subsequences. \square

More general problems of kind (26) can be discretized and their convergence can be proved in much the same spirit; for the elliptic case, see [10, 15, 30] and [26] for the cases of x -dependent and u -dependent Leray-Lions type nonlinearities $\varphi(x, u, \nabla u)$, respectively.

4.2. A parabolic-elliptic “bidomain” cardiac model. In this section, we describe another problem that motivated the analysis tools for CeVe-DDFV schemes presented in the previous sections.

The bidomain model, originating in [48], provides a description of the cardiac electric activity by means of two potentials: intercellular (u_i) and extracellular (u_e), as well as of their difference $v = u_i - u_e$. It uses auxiliary “gating variables”, governed by stiff ordinary differential equations, in order to simulate the “ionic current” term which depends on v in a non-local in time way. For a study of space discretization, a simplified model was introduced in [13] (see [14] for a first finite volume study on the meshes of [28]) where the ionic current $H[v]$ is just a local function of v (nonetheless, such a simplification allows to mimic, to a certain extent, the depolarization sequence in the cardiac tissue, taking the ionic current term $H[v]$ to be a cubic polynomial); this model writes

$$(37) \quad \begin{cases} v_t - \operatorname{div}(\mathcal{M}_i(x) \nabla u_i) + H(v) = I_{ap}, & \text{in } Q = (0, T) \times \Omega, \\ v_t + \operatorname{div}(\mathcal{M}_e(x) \nabla u_e) + H(v) = I_{ap}, & \text{in } Q, \end{cases}$$

where $\mathcal{M}_{i,e}$ are positive definite space-dependent matrices (they are anisotropic due to the fiber structure of the heart muscle); I_{ap} is an L^2 “applied current” which is the forcing term; and there is an initial condition $v_0 \in L^2(\Omega)$ for v and boundary conditions (in the simplest case, the Neumann ones) for u_i, u_e . For the nonlinearity h , it is assumed that

$$\frac{1}{C}|v|^r - Cv^2 \leq H(v)v \leq C(1 + |v|^r) \quad \text{for some constant } C > 0 \text{ and } r > 2;$$

the practical case is $r = 4$. The domain Ω is three-dimensional, but the 2D case (corresponding to slices of the heart) is also of interest. It should be emphasized that the goal of the simulation is to reproduce, in the mean, the very rapid transitions (polarization-depolarization sequences) occurring in the heart; the indicators of interest include, e.g., the depolarization front propagation velocity (see e.g. [5]). Further work is needed to couple these electrical phenomena with elastic contractions of the heart muscle.

The use of CeVe-DDFV schemes fo (37) and the simpler (“monodomain”) model was initiated by Ch. Pierre in his thesis [47]. The scheme, which is very similar to the ours (the gradient reconstruction is the same; the only difference is in the discretization of the source terms) was applied to the bidomain equations in [22, 23]. In [5], based on the above presentation of the 3D CeVe-DDFV scheme, two finite volume schemes for (37) are studied from the point of view of convergence. Writing of the schemes is straightforward; e.g., the first equation in (37) is approximated by

$$\frac{v^{\bar{x},n} - v^{\bar{x},n-1}}{\Delta t} - \operatorname{div}^{\bar{x}}[\mathcal{M}_i^{\bar{x}} \nabla^{\bar{x}} u_i^{\bar{x},n}] + H^{\bar{x},n} - I_{ap}^{\bar{x},n} = 0,$$

where $\mathcal{M}_i^{\bar{x}}$ is the constant per diamond projection of \mathcal{M}_i , $I_{ap}^{\bar{x},n}$ is the projection of the source term on the CeVe-DDFV mesh, and $H^{\bar{x},n}$ is the $v^{\bar{x},\Delta t}$ -dependent ionic current term (this point be specified in more detail). Further, the Neumann boundary condition is taken into account into the definition of the discrete divergence. More precisely, there are no boundary volumes for this scheme; additional unknowns are introduced on the boundary, so that the space $\mathbb{R}_0^{\bar{x}}$ is replaced

by the space not including the boundary conditions, and additional equations for these unknowns are obtained from the balance of the flux, given by the scheme, with the boundary flux prescribed for $\mathcal{M}_i(x) \nabla u_i$. We refer to [5] for details of the construction and for the discrete duality formula taking into account non-zero boundary conditions.

What is to be made precise is the discretization of the ionic current term $H^{\mathfrak{x},n}$ at time step n . In [5], we made the following two choices:

- (Fully implicit scheme) $H^{\mathfrak{x},n} := (H(v))^{\mathfrak{x},n}$;
- (Linearized scheme) for the sake of simplicity of presentation, assume $zH(z) \geq 0$, thus $H(z) = z\tilde{H}(z)$; then we pick $H^{\mathfrak{x},n} := (\tilde{H}(v))^{\mathfrak{x},n-1} v^{\mathfrak{x},n}$.

Here, $(H(v))^{\mathfrak{x},n}$ denotes the re-projection, on the CeVe-DDFV mesh \mathfrak{T} , of the function

$$\frac{1}{3}H(v^{\mathfrak{m}^o,n}) + \frac{2}{3}H(v^{\mathfrak{m}^*,n})$$

(with $v^{\mathfrak{m}^o,n}$ and $v^{\mathfrak{m}^*,n}$ the two components of $v^{\mathfrak{x},n}$), according to formula (51) in Appendix C below. The meaning of $(\tilde{H}(v))^{\mathfrak{x},n-1}$ is analogous. The technical reasons leading to this choice are presented in Appendix C.

It is understood that the first scheme is nonlinear, thus making appeal to heavier implementation schemes; the second scheme is linear, but it leads to weaker *a priori* estimates and its convergence is therefore more difficult to analyze. Convergence proof for the fully implicit, nonlinear scheme uses (in a somewhat simpler setting) the same arguments as in the proof of Theorem 4.2. Notice that L^2 -based compactness tools, in the spirit of [1] and [28], can replace the use of Proposition 3.11, (indeed, the estimates on discrete ionic current term allow for multiplying $H^{\mathfrak{x},\Delta t}$ by an $L^r(Q)$ function). Yet the study of the linearized scheme requires the use of the Sobolev embeddings of Proposition 3.4 or Remark 3.5, and the resulting integrability is just $H^{\mathfrak{x},\Delta t} \in L^1(Q)$ for $r \leq 4$ (in dimension three). Thus the L^1 -based Proposition 3.11 appears as an optimal tool for proving space-time compactness of $(v^{\mathfrak{x}_h,\Delta t_h})_h$. To conclude the proof, an equi-integrability of $(H^{\mathfrak{x}_h,\Delta t_h})_h$ is needed, which leads to the restriction $r < 4$ in dimension three of which the practical case is the borderline (in $2D$, the practical case $r = 4$ is covered by the analogous proof).

Numerical results on problem (37) are presented and commented in [5].

4.3. Degenerate convection-diffusion problems and discrete entropy dissipation. The DDFV schemes were initially designed as one among many other solutions to the problem of approximating anisotropic diffusion problems or even isotropic problems on general meshes (Hermeline [40, 39, 41, 42], Domelevo and Omnès [25], Pierre et al. [47, 24]). They turned out to be well suited for nonlinear diffusion problems ([10, 15, 19] and the above Section 4.1). The common feature here is that these problems are analyzed using variational techniques, i.e. using the solution itself as the test function. The discrete duality feature therefore allowed for getting energy conservation properties that lead to *a priori* estimates; with the estimates (and thus the weak compactness properties) in hand, one recasts the scheme under the weak form (see Proposition 4.1 in Section 4.1; cf. [5]) and thus proves convergence.

Many important applications, such as nonlinear degenerate parabolic problems of convection-diffusion type

$$(38) \quad u_t - \operatorname{div}(\varphi(\nabla A(u)) - F(u)) = 0$$

(with A continuous, increasing but non-strictly increasing, and with $\varphi(\cdot)$ of the kind (27)) require the use of *nonlinear* test functions and of *dissipation inequalities* in the place of energy conservation identities. The same is true for linear problems analyzed by nonlinear methods, such as generalized solutions of $-\Delta u = f$ with L^1 or measure datum f (see Gallouët et al. [33],[27] and references therein). In both cases, the analysis methods heavily rely on nonlinear chain rule arguments, that are not natural in the discrete setting.

While e.g. the DDFV discretization of the diffusion term appears as suitable in both cases (and on quite general meshes, as it was the case in Sections 4.1,4.2), the tools of stability and convergence analysis seem to require the orthogonality condition on the meshes, in order to get appropriate “chain rule kind”-inequalities. Indeed, in the previous works on the subject the

condition $\overline{x_K x_L} \perp \kappa|L$ was always exploited (see [33, 27] for the linear case, and [31, 3] for the case (38)). The schemes of [33, 27, 31] are two-point schemes in the spirit of Eymard, Gallouët and Herbin [28] (the diffusion being linear and isotropic in these cases); while in [3], the diffusion is nonlinear and therefore, an “orthogonal” DDFV scheme, in 3D and in 2D, was used. Let us point out the key ingredient of the convergence analysis of [3], which can be seen as a discrete entropy dissipation inequality for diffusion terms. Notice that a discrete maximum principle for DDFV approximations of (38) is deduced from this result.

Proposition 4.3. (see Andreianov, Bendahmane and Karlsen [3])

Let \mathfrak{T} be a DDFV mesh in 2D or in 3D; in the latter case, assume all the primal interfaces $\kappa|L$ are triangles. Impose the following orthogonality restriction:

for all neighbours K, L (resp., K^*, L^*) there holds $\overline{x_K x_L} \perp \kappa|L$ (resp., $\overline{x_{K^*} x_{L^*}} \perp \kappa^*|L^*$),

and assume that $\varphi(\xi) = k(|\xi|)\xi$ with a nonnegative (possibly singular at zero) function $k(\cdot)$. Let A be a continuous nondecreasing function on \mathbb{R} ; given a non-decreasing function θ on \mathbb{R} , set $A_\theta(z) = \int_0^z \theta(s) dA(s)$.

Let $u^\mathfrak{T} \in \mathbb{R}_0^\mathfrak{T}$ and $\psi^\mathfrak{T} \in \mathbb{R}_0^\mathfrak{T}$ (the zero boundary condition for $\psi^\mathfrak{T}$ can be replaced by the requirement $\theta(0) = 0$), with $\psi^\mathfrak{T} \geq 0$. Then the following “dissipative chain rule property” holds:

$$(39) \quad \left[\operatorname{div}^\mathfrak{T} [k(\nabla^\mathfrak{T} A(u^\mathfrak{T})) \nabla^\mathfrak{T} A(u^\mathfrak{T})], \theta(u^\mathfrak{T}) \psi^\mathfrak{T} \right]_\Omega \leq - \left\{ k(\nabla^\mathfrak{T} A(u^\mathfrak{T})) \nabla^\mathfrak{T} A_\theta(u^\mathfrak{T}), \nabla^\mathfrak{T} \psi^\mathfrak{T} \right\}_\Omega.$$

Inequality (39) comes from the convexity inequality that replaces the chain rule $A'(z)\theta(z) = (A_\theta)'(z)$:

$$(A(z) - A(\hat{z}))\theta(\hat{z}) \leq A_\theta(z) - A_\theta(\hat{z}) \quad \text{for all } z, \hat{z} \in \mathbb{R}.$$

The proof is straightforward: it uses the summation-by-parts procedure, the particular structure $\varphi(\xi) = k(|\xi|)\xi$ of $\varphi(\cdot)$ which is, in particular, isotropic, and also the particular expression of the discrete gradient under the orthogonality condition that avoids mixing the primal and the dual unknowns (except in the term $k(\nabla^\mathfrak{T} A(u^\mathfrak{T}))$ that is not transformed). In absence of the orthogonality condition (or for anisotropic φ) we are not aware of any proof of properties that could play the role of (39) in the convergence analysis for (38).

5. NUMERICAL RESULTS FOR ELLIPTIC-PARABOLIC PROBLEMS

We illustrate the convergence behaviour of the CeVe-DDFV scheme for the parabolic problem (26) in two situations. Test 1 corresponds to a linear anisotropic problem, whereas Test 2 is a fully non linear one.

<p>Test 1</p> $b = Id$ $\varphi(\xi) = A\xi, \text{ with } A = \begin{pmatrix} 1 & 0.5 & 0 \\ 0.5 & 1 & 0 \\ 0 & 0.5 & 1 \end{pmatrix}$	<p>Test 2</p> $b(s) = \frac{1}{2}(1 - \cos(\pi s))\mathbf{1}_{[0,1]}(s) + \mathbf{1}_{[1,+\infty]}(s)$ $\varphi(\xi) = \xi ^{p-2}\xi, \text{ with } p = 3$
------------------------------------------------------------------------------------------------------------------------------------------------	--------------------------------------------------------------------------------------------------------------------------------------------------------------------

The tests are performed in the 3D unit square, on three families of meshes: cubic meshes, tetrahedral meshes and prismatic meshes with general faces as illustrated in Figure 3. We take the exact solution $u(t, x) = v(t)w(x, y, z) = e^{-t} \sin(\pi x) \sin(\pi y) \sin(\pi z)$ (now (x, y, z) denotes a generic point of the unit cube), with the homogeneous Dirichlet boundary condition (note that $w|_{\partial\Omega} = 0$), and we calculate the source term corresponding to the solution u of (26). The penalization operator used in the convergence proof of Section 4.1, is omitted. In case of Test 2, the scheme is nonlinear; it is solved thanks to the decomposition-coordination algorithm described in Appendix D.

Accuracy of the scheme. To put the discrete and the exact solutions “at the same level”, we use the projection $\mathbb{P}^\mathfrak{T}u_e$ of the exact solution and the associated discrete gradient reconstruction $\overline{\nabla}^\mathfrak{T}\mathbb{P}^\mathfrak{T}u_e$. The $L^p(0, T; L^p(\Omega))$ norm of the error $\mathcal{E}^\mathfrak{T} := u^\mathfrak{T} - \mathbb{P}^\mathfrak{T}u_e$ ($p = 2$ for Test 1), as well as

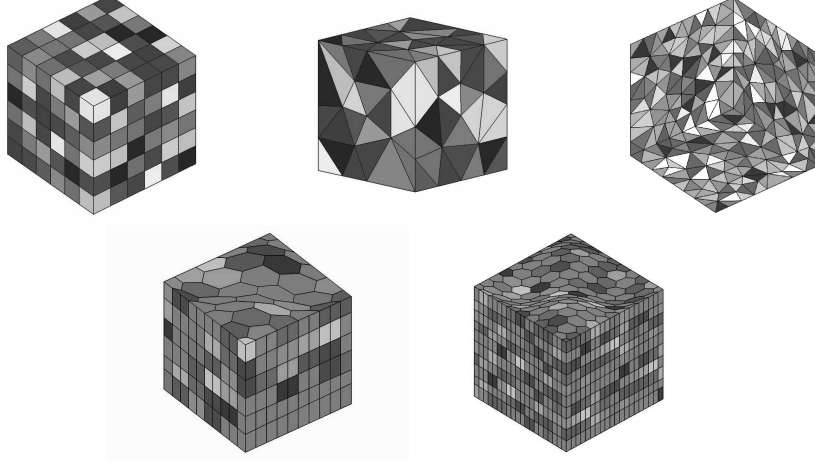


FIGURE 3. Cubic mesh level 0 (6x6x6), Tetrahedral meshes level 0 and level 1, Prismatic meshes level 0 (5x5x5) and level 1 (10x10x10)

Mesh level	Δt	$\ \tilde{\mathcal{E}}\ _{L^p(L^p)}$	rate	$\ \overrightarrow{\nabla}^{\mathfrak{x}} \tilde{\mathcal{E}}\ _{L^p(L^p)}$	rate	$\ \delta^{\mathfrak{x}} b\ _{L^\infty(L^1)}$	rate
0 - 6x6x6	5.0E-02	0.455E-01	-	0.520E-01	-	0.390E-01	-
1 - 9x9x9	2.4E-02	0.198E-01	1.933	0.228E-01	1.918	0.174E-01	1.878
2 - 12x12x12	1.25E-02	0.111E-01	1.938	0.127E-01	1.931	0.979E-02	1.905
3 - 18x18x18	5.07E-03	0.488E-02	1.951	0.564E-02	1.947	0.436E-02	1.933
4 - 24x24x24	2.79E-03	0.274E-02	1.962	0.317E-02	1.960	0.245E-02	1.953

TABLE 1. Test 1-Cubic meshes

Mesh level	Δt	$\ \tilde{\mathcal{E}}\ _{L^p(L^p)}$	rate	$\ \overrightarrow{\nabla}^{\mathfrak{x}} \tilde{\mathcal{E}}\ _{L^p(L^p)}$	rate	$\ \delta^{\mathfrak{x}} b\ _{L^\infty(L^1)}$	rate
0	5.0E-02	0.856E-01	-	0.164E+00	-	0.774E-01	-
1	1.16E-02	0.187E-01	1.998	0.685E-01	1.148	0.154E-01	2.122
2	7.02E-03	0.117E-01	2.072	0.535E-01	1.098	0.103E-01	1.799
3	4.42E-03	0.742E-02	1.987	0.396E-01	1.308	0.671E-02	1.850
4	2.79E-03	0.485E-02	1.852	0.313E-01	1.015	0.445E-02	1.786

TABLE 2. Test 1-Tetrahedral meshes

Mesh	Δt	$\ \tilde{\mathcal{E}}\ _{L^p(L^p)}$	rate	$\ \overrightarrow{\nabla}^{\mathfrak{x}} \tilde{\mathcal{E}}\ _{L^p(L^p)}$	rate	$\ \delta^{\mathfrak{x}} b\ _{L^\infty(L^1)}$	rate
0 - 5x5x5	5.0E-02	0.462E-01	-	0.584E-01	-	0.418E-01	-
1 - 10x10x10	1.51E-02	0.143E-01	1.886	0.202E-01	1.710	0.134E-01	1.831
2 - 15x15x15	6.18E-03	0.631E-02	1.916	0.101E-01	1.617	0.595E-02	1.895

TABLE 3. Test 1-Prismal meshes with general faces

the $L^\infty(0.T; L^p(\Omega))$ norm of the gradient $\overrightarrow{\nabla}^{\mathfrak{x}} \tilde{\mathcal{E}} := \overrightarrow{\nabla}^{\mathfrak{x}} u^{\mathfrak{x}} - \overrightarrow{\nabla}^{\mathfrak{x}} \mathbb{P}^{\mathfrak{x}} u_e$ and the $L^\infty(0.T; L^1(\Omega))$ of $\delta^{\mathfrak{x}} b = b(u^{\mathfrak{x}}) - b(\mathbb{P}^{\mathfrak{x}} u_e)$ are reported in Tables 1-5. We focus here on the accuracy of the diffusive part of the discrete operator. Therefore we have adapted the time step Δt to the size of the mesh by choosing $\Delta t_i = \Delta t_0((\#unknowns)_i/(\#unknowns)_0)^{\frac{1}{3}}$. Note that we obtain super-convergence for cubic meshes even in the nonlinear case; this was observed for other kinds of schemes (see, e.g., [9]).

Mesh level	Δt	$\ \tilde{\mathcal{E}}\ _{L^p(L^p)}$	rate	$\ \overline{\nabla^{\mathfrak{T}} \tilde{\mathcal{E}}}\ _{L^p(L^p)}$	rate	$\ \delta^{\mathfrak{T}} b\ _{L^\infty(L^1)}$	rate
0 - 6x6x6	5.0E-02	0.456E-01	-	0.497E-01	-	0.525E-01	-
1 - 9x9x9	2.4E-02	0.197E-01	1.950	0.217E-01	1.921	0.222E-01	1.993
2 - 12x12x12	1.25E-02	0.110E-01	1.942	0.122E-01	1.934	0.123E-01	1.976
3 - 18x18x18	5.07E-03	0.485E-02	1.952	0.539E-02	1.943	0.539E-02	1.965

TABLE 4. Test 2 : Cubic meshes

Mesh level	Δt	$\ \tilde{\mathcal{E}}\ _{L^p(L^p)}$	rate	$\ \overline{\nabla^{\mathfrak{T}} \tilde{\mathcal{E}}}\ _{L^p(L^p)}$	rate	$\ \delta^{\mathfrak{T}} b\ _{L^\infty(L^1)}$	rate
0 - 5x5x5	5.0E-02	0.472E-01	-	0.588E-01	-	0.593E-01	-
1 - 10x10x10	1.51E-02	0.143E-01	1.922	0.214E-01	1.626	0.175E-01	1.961
2 - 15x15x15	6.18E-03	0.620E-02	1.950	0.115E-01	1.456	0.765E-02	1.939

TABLE 5. Test 2-Prismal meshes with general faces

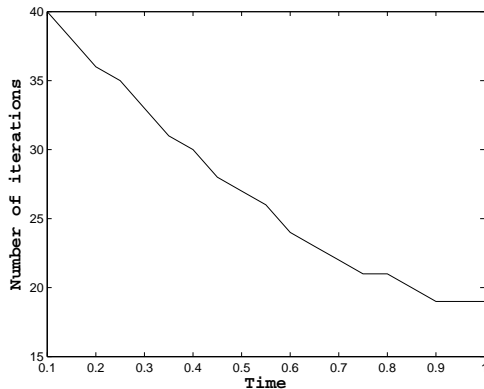


FIGURE 4. Number of iterations of the decomposition coordination algorithm for Test 2 (Prismatic mesh level 0 is used).

Behaviour the decomposition coordination algorithm. We fixed here the value of the penalization parameters r and γ to 1. Optimal choice of this parameters will not be investigated here. The number of iterations of the decomposition coordination decreases with time, as it is shown in Figure 4 (with the tolerance tol that has been fixed to 10^{-5}). Note that no more than three iterations are needed in the Newton steps of the algorithm.

6.A. APPENDIX A: AN L^1 SPACE-AND-TIME COMPACTNESS LEMMA

Before turning to the proof, let us mention that in view of the uniform $L^1((0, T) \times \Omega)$ bound on the two components of $b(u^{\mathfrak{T}_h, \Delta t_h})$, the assumption that the components of $(b(u^{\mathfrak{T}_h, 0}))_h$ are bounded in $L^1(\Omega)$ is clearly not essential (yet, it is not restrictive in practice). The only purpose of the assumption that $u^{\mathfrak{T}_h, \Delta t_h}$ are zero in the boundary volumes of \mathfrak{T}_h is to make trivial the issue of extension of $u^{\mathfrak{T}_h, \Delta t_h}$ in space to a small neighbourhood of Ω .

To stress the three aspects of the meshing that are important for the below proof, firstly, let us recall that the assumption $l = 3$ yields the bounds (14) that we rewrite as

$$(40) \quad \frac{|w_L - w_K|}{d_{KL}} \leq |\nabla_s w^{\mathfrak{T}}|, \quad \frac{|w_{L^*} - w_{K^*}|}{d_{K^*L^*}} \leq |\nabla_s w^{\mathfrak{T}}|$$

for $s = S_{K^*|L^*}^{KL}$. Secondly, notice that the construction of the discrete gradient and the assumptions (7) and (8) permit to get the bound

$$(41) \quad \forall w^o, w^* \in \mathcal{D}(\Omega) \quad \left\| \nabla^{\mathfrak{T}}(\mathbb{P}^{\mathfrak{M}^o_h} w^o, \mathbb{P}^{\mathfrak{M}^*_h} w^*) \right\|_{L^\infty(\Omega)} \leq C(\text{reg}(\mathfrak{T})) \left(\|\nabla w^o\|_{L^\infty(\Omega)} + \|\nabla w^*\|_{L^\infty(\Omega)} \right).$$

Thirdly, note that the discrete duality property readily yields the bound

$$(42) \quad \forall w^{\mathfrak{T}} \in \mathbb{R}_0^{\mathfrak{T}} \quad \forall \vec{\mathcal{F}}^{\mathfrak{T}} \in (\mathbb{R}^3)^{\mathfrak{D}} \quad \left| \left[-\text{div}^{\mathfrak{T}} \vec{\mathcal{F}}^{\mathfrak{T}}, w^{\mathfrak{T}} \right]_{\Omega} \right| \leq \|\nabla^{\mathfrak{T}} w^{\mathfrak{T}}\|_{L^\infty(\Omega)} \|\vec{\mathcal{F}}^{\mathfrak{T}}\|_{L^1(\Omega)}.$$

PROOF OF PROPOSITION 3.11: The proof is divided into four steps, the heart of it being Step 3.

First, let us fix some notation. Set $Q_T := (0, T) \times \Omega$. We will denote by $u^{h,o}(t, x)$, $u^{h,*}(t, x)$ the components

$$u^{h,o}(t, x) := \sum_{n=1}^{N_{\Delta t_h}} u^{\mathfrak{M}^o_h, n}(x) \mathbb{1}_{((n-1)\Delta t_h, n\Delta t_h]}(t), \quad u^{h,*}(t, x) := \sum_{n=1}^{N_{\Delta t_h}} u^{\mathfrak{M}^*_h, n}(x) \mathbb{1}_{((n-1)\Delta t_h, n\Delta t_h]}(t)$$

of the discrete solution. These functions are extended by the constant in t values $u^{\mathfrak{M}^o_h, N_{\Delta t_h}}(x)$, $u^{\mathfrak{M}^*_h, N_{\Delta t_h}}(x)$ on $(N_{\Delta t_h} \Delta t_h, +\infty)$, then they are extended by zero on $(0, +\infty) \times (\mathbb{R}^3 \setminus \Omega)$ (notice that both extensions do not introduce additional jumps).

Step 1 : Property (40) and the uniform estimate (25) of the discrete gradient imply the uniform local estimate of the space translates of u^h : the space translates of $u^{h,o}$ obey

$$(43) \quad \sup_{|\Delta x| \leq \Delta} \int_0^T \int_{\mathbb{R}^3} |u^{h,o}(t, x + \Delta x) - u^{h,o}(t, x)| \, dx dt \leq \Delta M C(\text{reg}(\mathfrak{T}_h)),$$

and the identical estimate holds for $u^{h,*}$.

The proof of (43) is standard; we give it here for the sake of completeness. A shorter proof can be derived from the arguments of [29, Lemma 5.1] (it is justified in this lemma that discrete $W^{1,1}$ estimates are in fact BV estimates, and therefore the standard translation properties of the BV functions can be used).

For $x \in \mathbb{R}^3$ and an interface $K|L$ of the mesh \mathfrak{M}^o_h , set $\bar{\psi}_{K|L}(x) = 1$, in case the segment $[x, x + \Delta x]$ crosses $K|L$, and $\bar{\psi}_{K|L}(x) = 0$ otherwise. Note that $\int_{\mathbb{R}^3} \bar{\psi}_{K|L}(x) \, dx \leq m_{K|L} \Delta$. Using (40) and property

$$\text{reg}(\mathfrak{T}_h) \text{Vol}(S_{K^*|L^*}^{KL}) \geq m_{K|L} d_{KL}$$

that comes from the inclination bound (8), we have

$$\begin{aligned} \int_0^T \int_{\Omega} |u^h(t, x) - u^h(t, x + \Delta x)| \, dx dt &\leq \sum_{n=0}^{N_{\Delta t_h}} \sum_{s \in \mathfrak{E}} \Delta t_h |u_K^n - u_L^n| \int_{\Omega} \bar{\psi}_{K|L}(x) \, dx \\ &\leq \Delta \sum_{n=0}^{N_{\Delta t_h}} \Delta t_h \sum_{S \in \mathfrak{E}} m_{K|L} |u_K^n - u_L^n| \leq \Delta \sum_{n=0}^{N_{\Delta t_h}} \Delta t_h \sum_{S \in \mathfrak{E}} m_{K|L} d_{KL} |\nabla_s u^{\mathfrak{T}_h, n}| \\ &\leq \text{reg}(\mathfrak{T}_h) \Delta \sum_{n=1}^{N_{\Delta t_h}} \Delta t_h \sum_{S \in \mathfrak{E}} \text{Vol}(s) |\nabla_s u^{\mathfrak{T}_h, n}|, \end{aligned}$$

meaning as usual that the summation runs over all the subdiamonds $s = S_{K^*|L^*}^{KL}$. The right-hand side of the above inequality is exactly $\text{reg}(\mathfrak{T}_h) \Delta \sum_{n=1}^{N_{\Delta t_h}} \Delta t_h \|\nabla^{\mathfrak{T}_h} u^{\mathfrak{T}_h, n}\|_{L^1(\Omega)}$, and we conclude using (25).

The same arguments yield the space translation estimate on $u^{h,*}$.

Step 2 : We replace the study of $u^{h,o}, u^{h,*}$ (constant per cylinder $Q_K^n := K \times ((n-1)\Delta t_h, n\Delta t_h)$ or $Q_{K^*}^n := K^* \times ((n-1)\Delta t_h, n\Delta t_h)$) by the study of functions $\bar{u}^{h,o}, \bar{u}^{h,*}$ continuous in t for all x , constant in x for all volume K or K^* , defined via

$$\begin{aligned} b(\bar{u}^{h,o})(t, x) &= \sum_{n=1}^{N_{\Delta t_h}} \sum_{K \in \mathfrak{M}_h^{o_h}} \frac{1}{\Delta t_h} \left((t - (n-1)\Delta t_h)b(u_K^n) + (n\Delta t_h - t)b(u_K^{n-1}) \right) \mathbb{1}_{Q_K^n}(t, x), \\ \bar{b}(u^{h,*})(t, x) &= \sum_{n=1}^{N_{\Delta t_h}} \sum_{K^* \in \mathfrak{M}_h^{*h}} \frac{1}{\Delta t_h} \left((t - (n-1)\Delta t_h)b(u_{K^*}^n) + (n\Delta t_h - t)b(u_{K^*}^{n-1}) \right) \mathbb{1}_{Q_{K^*}^n}(t, x). \end{aligned}$$

We also extend $\bar{u}^{h,o}, \bar{u}^{h,*}$ by the constant in time values $u^{\mathfrak{M}_h^{o_h}, N_{\Delta t_h}}, u^{\mathfrak{M}_h^{*h}, N_{\Delta t_h}}$ on $(N_{\Delta t_h}\Delta t_h, +\infty)$. Similarly, we introduce the functions $f^h, f^{h,*}$ and $\bar{\mathcal{F}}^h$ in $L^1(Q_T)$; moreover, we define

$$\operatorname{div}^{h,o} \bar{\mathcal{F}}^h := \sum_{n=1}^{N_{\Delta t_h}} \sum_{K \in \mathfrak{M}_h^{o_h}} \operatorname{div}_K \bar{\mathcal{F}}^{\varpi, n} \mathbb{1}_{Q_K^n}(t, x), \quad \operatorname{div}^{h,*} \bar{\mathcal{F}}^h := \sum_{n=1}^{N_{\Delta t_h}} \sum_{K^* \in \mathfrak{M}_h^{*h}} \operatorname{div}_{K^*} \bar{\mathcal{F}}^{\varpi, n} \mathbb{1}_{Q_{K^*}^n}(t, x).$$

The functions, $f^h, f^{h,*}$ and $\bar{\mathcal{F}}^h, \operatorname{div}^{h,o} \bar{\mathcal{F}}^h, \operatorname{div}^{h,*} \bar{\mathcal{F}}^h$ are extended by zero from Q_T to $(0, +\infty) \times \mathbb{R}^3$.

Considering the t -dependent discrete functions $\bar{u}^{\varpi_h}(t)$ with the components $\bar{u}^{h,o}(t), \bar{u}^{h,*}(t)$ on the meshes \mathfrak{M}_h^o and \mathfrak{M}_h^* , we are in a position to rewrite the discrete equations (23) under the form

$$(44) \quad \frac{\partial}{\partial t} b(\bar{u}^{h,o}) = \operatorname{div}^{h,o} \bar{\mathcal{F}}^h + f^{h,o}, \quad \frac{\partial}{\partial t} b(\bar{u}^{h,*}) = \operatorname{div}^{h,*} \bar{\mathcal{F}}^h + f^{h,*}$$

where the equation is satisfied in $W^{1,1}(\mathbb{R}^+)$ in time, for a.e. $x \in \mathbb{R}^3$.

In addition, denoting by ω_b a concave modulus of continuity⁴ of b , by the definition of $\bar{u}^{h,o}$ and the Jensen inequality we have

$$\begin{aligned} & \int_0^{+\infty} \int_{\Omega} |b(\bar{u}^{h,o})(t, x + \Delta x) - b(\bar{u}^{h,o})(t, x)| dx dt \\ & \leq 2 \int_0^T \int_{\Omega} |b(u^{h,o})(t, x + \Delta x) - b(u^{h,o})(t, x)| dx dt + 2\Delta t_h \int_{\Omega} |b_0^{h,o}(x)| dx \\ & \leq T \operatorname{Vol}(\Omega) \omega_b \left(\frac{1}{T \operatorname{Vol}(\Omega)} \int_0^T \int_{\Omega} |u^{h,o}(t, x + \Delta x) - u^{h,o}(t, x)| dx dt \right) + 2\Delta t_h \int_{\Omega} |b_0^{h,o}(x)| dx, \end{aligned}$$

where $b_0^{h,o}(x) = \sum_{K \in \mathfrak{M}_h^{o_h}} b(u_K^0) \mathbb{1}_K(x)$ is the first component of the initial datum $b(u^{\varpi_h, 0})$.

By the result of Step 1, the assumption $\Delta t_h \rightarrow 0$ as $h \rightarrow 0$ and the uniform $L^1(\Omega)$ bound on $b(u^{\mathfrak{M}_h^{o_h}, 0})_h$, the space translates of $\bar{u}^{h,o}$ on $(0, T) \times \Omega$ are estimated uniformly for all sequence $(h_i)_i$ convergent to zero. In the same way, the space translates of $\bar{u}^{h,*}$ on $(0, T) \times \Omega$ are estimated.

Finally, $b(\bar{u}^{h_i, o}), b(\bar{u}^{h_i, *})$ are bounded in $L^1((0, T) \times \Omega)$ uniformly in i . Indeed, this comes from

$$\int_0^T \int_{\Omega} |b(\bar{u}^{h_i, o})(t, x)| dx dt \leq 2 \int_0^{\Delta t_h N_{\Delta t_h}} \int_{\Omega} |b(u^{h_i, o})(t, x)| dx dt + \Delta t_h \int_{\Omega} |b_0^{h_i, o}(x)| dx$$

(the identical estimate holds for $b(\bar{u}^{h_i, *})$) and from the assumptions of the proposition.

In the sequel, we drop the subscript i in the notation.

Step 3 : Now we adapt the idea of the Kruzhkov lemma ([44]). We show that, provided $\bar{u}^{h,o}, \bar{u}^{h,*}$ solve a discrete evolution equation of the form (44) with terms bounded in L^1 and an estimate of the space translates of $b(\bar{u}^{h,o}), b(\bar{u}^{h,*})$ is available, there is also a uniform estimate of the time translates of $b(\bar{u}^{h,o}), b(\bar{u}^{h,*})$:

$$(45) \quad \sup_{\theta \in (0, \tau]} \int_0^{+\infty} \int_{\Omega} \left(\frac{1}{3} \left| b(\bar{u}^{h,o})(t+\theta, x) - b(\bar{u}^{h,o})(t, x) \right| + \frac{2}{3} \left| b(\bar{u}^{h,*})(t+\theta, x) - b(\bar{u}^{h,*})(t, x) \right| \right) dx dt \leq \tilde{\omega}(\tau).$$

⁴If $b(\bar{u}^{h_i, o})$ are equi-integrable, a local modulus of continuity is enough.

Here $\tilde{\omega} : \mathbb{R}^+ \rightarrow \mathbb{R}^+$ is a modulus of continuity, i.e., a non-decreasing function such that $\lim_{\tau \rightarrow 0} \tilde{\omega}(\tau) = 0$.

Let us construct $\tilde{\omega}(\cdot)$ verifying (45). First fix h and fix $\theta \in (0, \tau]$. Denote by $I^h(\theta)$ the integral in the left-hand side of (45). For $t \geq 0$, set

$$w^{h,o}(t, \cdot) := b(\bar{u}^{h,o})(t + \theta, \cdot) - b(\bar{u}^{h,o})(t, \cdot), \quad w^{h,*}(t, \cdot) := b(\bar{u}^{h,*})(t + \theta, \cdot) - b(\bar{u}^{h,*})(t, \cdot).$$

Notice that $w^{h,o}(t, \cdot) \equiv 0$, $w^{h,*}(t, \cdot) \equiv 0$ for large t .

Take a standard family $(\rho_\delta)_\delta$ of mollifiers on \mathbb{R}^3 defined as $\rho_\delta(x) := \delta^{-3} \rho(x/\delta)$, where ρ is a Lipschitz continuous, nonnegative function supported in the unit ball of \mathbb{R}^3 , and $\int_{\mathbb{R}^3} \rho(x) dx = 1$. In particular, we have

$$|\nabla \rho_\delta| \leq \frac{C}{\delta^{3+1}}.$$

Here and throughout the proof, C will denote a generic constant independent of h and δ . For all $t > 0$, define the function $\varphi^{h,o}(t, \cdot) : \mathbb{R}^3 \rightarrow \mathbb{R}$ by $\varphi^{h,o}(t) := \rho_\delta * (\text{sign } w^{h,o}(t))$. In order to lighten the notation, we do not stress the dependence of $\varphi^{h,o}$ on δ . Define $\varphi^{h,*}(t)$ similarly, starting from $w^{h,*}(t)$.

Now discretize $\varphi^{h,o}(t, \cdot)$ on the mesh \mathfrak{M}_h^o by setting $\varphi^{\mathfrak{M}_h^o}(t) := \mathbb{P}^{\mathfrak{M}_h^o} \varphi^{h,o}(t, \cdot)$; recall that this means that

$$\varphi_K(t) = \frac{1}{\text{Vol}(K)} \int_K \varphi^{h,o}(t, x) dx.$$

Further, discretize $\varphi^{h,*}(t, \cdot)$ on the mesh \mathfrak{M}_h^* by setting $\varphi^{\mathfrak{M}_h^*}(t) := \mathbb{P}^{\mathfrak{M}_h^*} \varphi^{h,*}(t, \cdot)$. Denote by $\varphi^h(t)$ the discrete function on the CeVe-DDFV mesh \mathfrak{T}_h of Ω with the two components $\varphi^{\mathfrak{M}_h^o}(t), \varphi^{\mathfrak{M}_h^*}(t)$. Denote by $w^h(t)$ the discrete function on \mathfrak{T}_h with the components $w^{h,o}(t), w^{h,*}(t)$.

Now for all fixed t , we integrate equations (44) in $t \in [s, s + \theta]$, then take the scalar product $\llbracket \cdot, \cdot \rrbracket_\Omega$ of the result by $\varphi^{\mathfrak{T}_h}(t)$. Finally, we integrate the obtained equality in s over \mathbb{R}^+ to get

$$(46) \quad \int_0^{+\infty} \llbracket w^h(s), \varphi^h(s) \rrbracket_\Omega ds = \int_0^{+\infty} \int_s^{s+\theta} \llbracket \text{div}^{\mathfrak{T}_h} \vec{F}^h(t) + f^h(t), \varphi^h(s) \rrbracket_\Omega dt ds.$$

Denote by $I_\delta^h(\theta)$ the left-hand side of (46). Using property (42), the definitions of discrete norms and the Fubini theorem, we infer

$$I_\delta^h(\theta) \leq \theta \left(\|\nabla^{\mathfrak{T}_h} w^{\mathfrak{T}_h}\|_{L^\infty(\Omega)} \|\mathcal{F}^h\|_{L^1(Q_T)} + \max\{\|\varphi^{\mathfrak{M}_h^o}\|_{L^\infty(Q_T)}, \|\varphi^{\mathfrak{M}_h^*}\|_{L^\infty(Q_T)}\} \times (\|f^{h,o}\|_{L^1(Q_T)} + \|f^{h,*}\|_{L^1(Q_T)}) \right).$$

Now the $L^1([0, T] \times \Omega)$ bounds (24) on $(\mathcal{F}^h)_h, (f^{h,o})_h$ and $(f^{h,*})_h$, the bounds

$$|\varphi^{h,o}(t, \cdot)| \leq 1, \quad |\varphi^{h,*}(t, \cdot)| \leq 1, \quad |\nabla \varphi^{h,o}(t, \cdot)| \leq C/\delta^4, \quad |\nabla \varphi^{h,*}(t, \cdot)| \leq C/\delta^4$$

and property (41) yield the estimate

$$(47) \quad I_\delta^h(\Delta t) \leq \theta C(\text{reg}(\mathfrak{T}_h)) M (1 + \delta^{-4})$$

for all h and δ small enough, uniformly in h . Now, notice that, $w^{h,o}$ and $\varphi^{h,o}$ being constant per $K \in \mathfrak{M}_h^o$, by the definition of $\varphi_K(t)$ we have

$$\begin{aligned} \text{Vol}(K) (|w_K(t)| - w_K(t) \varphi_K(t)) &= \text{Vol}(K) |w^{h,o}(t, x)| - w_K(t) \int_K \varphi^{h,o}(t, x) dx \\ &= \int_K (|w^{h,o}(t, x)| - w^{h,o}(t, x) \varphi^{h,o}(t, x)) dx; \end{aligned}$$

the identical equality holds on dual volumes k^* . Therefore (recalling again the definition of $\llbracket \cdot, \cdot \rrbracket_\Omega$),

$$\begin{aligned} I^h(\theta) - I_\delta^h(\theta) &= \int_0^{+\infty} \int_\Omega \left(\frac{1}{3} (|w^{h,o}(t,x)| - w^{h,o}(t,x) \varphi^{h,o}(t,x)) \right. \\ &\quad \left. + \frac{2}{3} (|w^{h,*}(t,x)| - w^{h,*}(t,x) \varphi^{h,*}(t,x)) \right) dx dt. \end{aligned}$$

Starting from this point, the argument of Kruzhkov [44] applies exactly as for the “continuous” case. Note the key inequality, valid for all monotone b such that $b(0) = 0$:

$$\forall \alpha, \gamma \in \mathbb{R} \quad |\alpha| - \alpha \operatorname{sign} \gamma \leq 2|\alpha - \gamma|.$$

Setting $\sigma := (x-y)/\delta$, we upper bound $|I^h(\theta) - I_\delta^h(\theta)|$ by

$$\begin{aligned} &2 \int_0^{+\infty} \int_\Omega \int_{\mathbb{R}^3} \rho_\delta(x-y) \left(\frac{1}{3} |w^{h,o}(t,x) - w^{h,o}(t,y)| + \frac{2}{3} |w^{h,*}(t,x) - w^{h,*}(t,y)| \right) dy dx dt \leq \\ &\leq 2 \int_{\mathbb{R}^3} \rho(\sigma) \int_0^{+\infty} \int_\Omega \left(\frac{1}{3} |b(\bar{u}^{h,o})(t,x) - b(\bar{u}^{h,o})(t,x - \delta\sigma)| + \frac{2}{3} |b(\bar{u}^{h,*})(t,x) - b(\bar{u}^{h,*})(t,x - \delta\sigma)| \right) dx dt d\sigma; \end{aligned}$$

therefore if $\omega(\cdot)$ is the modulus of continuity controlling the space translates of $\bar{b}(u^{h,o})$ and of $\bar{b}(u^{h,*})$ in $L^1((0,T) \times \Omega)$, then

$$(48) \quad |I^h(\theta) - I_\delta^h(\theta)| \leq 2\omega(\delta).$$

Recall that, by Steps 1 and 2 of the proof, one can choose $\omega(\cdot)$ independent of h . Combining (47) with (48), we conclude that the function

$$\tilde{\omega}(\tau) := \inf_{\delta > 0} C \{ \tau(1 + \delta^{-4}) + 2\omega(\delta) \}$$

upper bounds the quantity $\sup_{\theta \in (0,\tau]} I^h(\theta)$. Because $\tilde{\omega}(\tau)$ tends to 0 as $\tau \rightarrow 0$, this proves (45).

Step 4 : By the Frechet-Kolmogorov compactness criterion, the relative compactness of $(b(\bar{u}^{h,o}))_h$ and $(b(\bar{u}^{h,*}))_h$ in $L^1((0,T) \times \Omega)$ is a consequence of the estimates of Steps 2 and 3. In order to conclude, it suffices to show that

$$\|b(u^{h,o}) - b(\bar{u}^{h,o})\|_{L^1((0,T) \times \Omega)} \rightarrow 0 \quad \text{and} \quad \|b(u^{h,*}) - b(\bar{u}^{h,*})\|_{L^1((0,T) \times \Omega)} \rightarrow 0$$

as $h \rightarrow 0$. An easy calculation shows that

$$\text{for all } \alpha, \gamma \in \mathbb{R}, \int_0^1 |\kappa\alpha + (1-\kappa)\gamma| d\kappa \geq \frac{1}{2}(|\alpha| + |\gamma|).$$

Applying this inequality to $\alpha := b(u^{\mathfrak{m}^o_h, n+1}) - b(u^{\mathfrak{m}^o_h, n})$, $\gamma := b(u^{\mathfrak{m}^o_h, n}) - b(u^{\mathfrak{m}^o_h, n-1})$, from the definition of \bar{u}^h we deduce

$$\int_0^T \int_\Omega |b(u^{h,o})(t,x) - b(\bar{u}^{h,o})(t,x)| dx dt \leq 2 \int_0^{T+\Delta t_h} \int_\Omega |b(\bar{u}^{h,o})(t+\Delta t_h, x) - b(\bar{u}^{h,o})(t,x)| dx dt.$$

The identical estimate holds with $b(u^{h,o}), b(\bar{u}^{h,o})$ replaced by $b(u^{h,*}), b(\bar{u}^{h,*})$. Since Δt_h tends to zero as $h \rightarrow 0$, estimate (45) of Step 3 implies that the right-hand side of the above inequality converges to zero as h tends to zero. This ends the proof of the proposition. \square

6.B. APPENDIX B: A PENALIZATION OPERATOR

Penalization of a DDFV scheme may be useful in order to guarantee that the two components of a discrete “double” function $w^{\mathfrak{x}_h}$ converge to the same limit.

Indeed, we have seen that in the context of Proposition 3.9, the two components $w^{\mathfrak{m}^o_h}, w^{\mathfrak{m}^*_h}$ of discrete functions $w^{\mathfrak{x}_h}$ with bounded discrete $W_0^{1,p}$ norm may converge to two distinct limits. This can complicate the analysis of the DDFV discretizations for certain PDEs (although the fact that the components $w^{\mathfrak{m}^o_h}, w^{\mathfrak{m}^*_h}$ converge to a common limit can be implied by the structure of the PDE considered; see [10] for one particular case). In the context of the work [3], this difficulty

turned out to be an obstacle for proving convergence of the DDFV scheme. Therefore the idea to penalize the differences $w_K - w_{K^*}$ for $K \cap K^* \neq \emptyset$ was introduced. Let us give some details.

On the set $\mathbb{R}^{\mathfrak{T}}$ of discrete functions $w^{\mathfrak{T}}$ on $\overline{\Omega}$, following [3] we define the operator $\mathcal{P}^{\mathfrak{T}}[\cdot]$ of “double” mesh penalization by

$$\mathcal{P}^{\mathfrak{T}} : w^{\mathfrak{T}} \in \mathbb{R}^{\mathfrak{T}} \mapsto \mathcal{P}^{\mathfrak{T}} w^{\mathfrak{T}} = \left((\mathcal{P}_K w^{\mathfrak{T}})_{K \in \mathfrak{M}^o}, (\mathcal{P}_{K^*} w^{\mathfrak{T}})_{K^* \in \mathfrak{M}^*} \right) \in \mathbb{R}^{\mathfrak{T}},$$

where the entries $\mathcal{P}_K w^{\mathfrak{T}}$, $\mathcal{P}_{K^*} w^{\mathfrak{T}}$ of the discrete function $\mathcal{P}^{\mathfrak{T}} w^{\mathfrak{T}}$ on Ω are given by

$$\begin{aligned} \mathcal{P}_K w^{\mathfrak{T}} &:= 2 \frac{1}{\text{size}(\mathfrak{T})} \frac{1}{\text{Vol}(K)} \sum_{K^* \in \overline{\mathfrak{M}^*}} \text{Vol}(K \cap K^*) (w_K - w_{K^*}); \\ \mathcal{P}_{K^*} w^{\mathfrak{T}} &:= \frac{1}{\text{size}(\mathfrak{T})} \frac{1}{\text{Vol}(K^*)} \sum_{K \in \overline{\mathfrak{M}^o}} \text{Vol}(K \cap K^*) (w_{K^*} - w_K). \end{aligned}$$

The definitions are designed to get the following summation-by-parts formula:

Proposition 6.1. *Let $w^{\mathfrak{T}} \in \mathbb{R}^{\mathfrak{T}}$ and $\varphi^{\mathfrak{T}} \in \mathbb{R}_0^{\mathfrak{T}}$. Then*

$$\left[\mathcal{P}^{\mathfrak{T}} w^{\mathfrak{T}}, \varphi^{\mathfrak{T}} \right]_{\Omega} = \frac{2}{3} \sum_{K \in \overline{\mathfrak{M}^o}, K^* \in \overline{\mathfrak{M}^*}} \text{Vol}(K \cap K^*) \frac{(w_K - w_{K^*})(\varphi_K - \varphi_{K^*})}{\text{size}(\mathfrak{T})}.$$

The proof is straightforward from the definitions of $\left[\cdot, \cdot \right]_{\Omega}$ in (2) and of the operator $\mathcal{P}^{\mathfrak{T}}$.

Notice that adding such a penalization term into discrete equations corresponds, roughly speaking, to adding a small amount of discrete diffusion (e.g. on the uniform cartesian DDFV meshes of Section 2.2, the penalization operator is in fact a $\text{size}(\mathfrak{T})$ -small multiple of a discrete Laplacian). Therefore it is clear that this additional term does not affect the convergence of the schemes. In addition, except in some degenerate situations (e.g. on the meshes satisfying the orthogonality condition, the equations corresponding to primal and dual volumes are actually not coupled) adding this term does not enlarge the stencil of the scheme.

Adding the penalization leads to an additional estimate on discrete solutions that can be used as follows.

Proposition 6.2. *In the assumptions of Proposition 3.9, let us require in addition that*

$$(49) \quad \left[\mathcal{P}^{\mathfrak{T}_h} w^{\mathfrak{T}_h}, w^{\mathfrak{T}_h} \right]_{\Omega} \leq \text{const}$$

*uniformly in h . Then (upon extraction of convergent subsequences) the limits of the families $(w^{\mathfrak{M}^o_h})_h$ and $(w^{\mathfrak{M}^*_h})_h$ coincide.*

The proof is straightforward (see [3]).

In a similar manner, for the case of cartesian meshes one could penalize the differences between the neighbour values on $K^* \in \mathfrak{c}_h^*$ and on $K^* \in \mathfrak{o}_h^*$, to ensure that $w^{\mathfrak{M}^{\mathfrak{c},h}}$ and $w^{\mathfrak{M}^{\mathfrak{o},h}}$ converge to the same limit (notice that in case of such penalization, the example of Remark 3.8 would not be compatible with the uniform estimate (49)).

6.C. APPENDIX C: DDFV DISCRETIZATION OF REACTION TERMS

Recall that (unless the penalization technique of the previous paragraph is used) the two components $w^{\mathfrak{M}^o_h}$, $w^{\mathfrak{M}^*_h}$ of discrete functions $w^{\mathfrak{T}_h}$ may converge to two distinct limits w^o, w^* . Therefore, discretizing a function $\Psi := \psi(w)$ on \mathfrak{T} in the most straightforward way, namely

$$\Psi^{\mathfrak{T}} := \left((\psi(w_K))_{K \in \mathfrak{M}^o}, (\psi(w_{K^*}))_{K^* \in \mathfrak{M}^*} \right)$$

may lead to a difficulty. Indeed, at the limit e.g. of $I_h := \left[(\psi(w))^{\mathfrak{T}_h}, w^{\mathfrak{T}_h} \right]_{\Omega}$ we will find (see the definition (2) of the scalar product on $\mathbb{R}^{\mathfrak{T}}$)

$$(50) \quad \int_{\Omega} \left(\frac{1}{3} \psi(w^o) w^o + \frac{2}{3} \psi(w^*) w^* \right).$$

Because we have seen that the function $\frac{1}{3}w^o + \frac{2}{3}w^*$ should be considered as the natural limit of $w^{\mathfrak{x}_h}$ (namely, $\nabla^{\mathfrak{x}_h} w^{\mathfrak{x}_h}$ converges to the gradient of this function), as long as we cannot prove that $w^o = w^*$ we need to find

$$I := \int_{\Omega} \psi\left(\frac{1}{3}w^o + \frac{2}{3}w^*\right) \left(\frac{1}{3}w^o + \frac{2}{3}w^*\right).$$

at the limit of I_h , in the place of (50). Therefore we suggest that either penalization operators (see Appendix B) be used in order to enforce the equality $w^o = w^*$; or that the reaction terms be discretized on a 3D CeVe-DDFV mesh by taking, for discretization of $\Psi = \psi(w)$, the expression

$$(51) \quad \Psi^{\mathfrak{x}} := \left((\psi(\check{w}_K))_{K \in \mathfrak{M}^o}, (\psi(\check{w}_{K^*}))_{K^* \in \mathfrak{M}^*} \right),$$

$$\check{w}_K := \frac{1}{3}w^K + \frac{2}{3} \sum_{K^* \in \overline{\mathfrak{M}^*}} \frac{\text{Vol}(K \cap K^*)}{\text{Vol}(K)} w_{K^*}, \quad \check{w}_{K^*} := \frac{1}{3} \sum_{K \in \overline{\mathfrak{M}^o}} \frac{\text{Vol}(K \cap K^*)}{\text{Vol}(K^*)} w^K + \frac{2}{3} w_{K^*}$$

In other words, \check{w}_K and \check{w}_{K^*} are the mean values of the function $\frac{1}{3}w^{\mathfrak{M}^o} + \frac{2}{3}w^{\mathfrak{M}^*}$ on K and on K^* , respectively. With this choice, we have for all $w^{\mathfrak{x}} \in \mathbb{R}_0^{\mathfrak{x}}$, for all $\varphi^{\mathfrak{x}} \in \mathbb{R}^{\mathfrak{x}}$,

$$\left[(\psi(w))^{\mathfrak{x}}, \varphi^{\mathfrak{x}} \right]_{\Omega} = \int_{\Omega} \psi\left(\frac{1}{3}w^{\mathfrak{M}^o} + \frac{2}{3}w^{\mathfrak{M}^*}\right) \left(\frac{1}{3}\varphi^{\mathfrak{M}^o} + \frac{2}{3}\varphi^{\mathfrak{M}^*}\right).$$

Notice that in the case of general meshes, such treatment of reaction terms does not enlarge the stencil of a DDFV scheme used for the discretization of a diffusion operator.

One example of the use of (51) is given in [5] and in Section 4.2 below.

Notice that this approach to discretization of reaction terms is particularly natural if the DDFV scheme is viewed as a “gradient scheme” in the sense of Eymard, Herbin and Guichard [32], because in this case the unknown discrete solution in the scheme is approximated via a lifted function that, in our case, takes precisely the form $\frac{1}{3}w^{\mathfrak{M}^o} + \frac{2}{3}w^{\mathfrak{M}^*}$.

Remark 6.3. Note that, instead of adding the penalization operator in the scheme (28), one could treat the time evolution term in (28) using the discretization of type (51) for $b(u)$.

6.D. APPENDIX D: THE COORDINATION-DECOMPOSITION ALGORITHM

The goal is to solve the nonlinear system

$$b(u^{\mathfrak{x},n}) - \Delta t \operatorname{div}^{\mathfrak{x}} \varphi(\nabla^{\mathfrak{x}} u^{\mathfrak{x},n}) = b(u^{\mathfrak{x},n-1}) + \Delta t f^{\mathfrak{x},n}$$

(in the numerical tests, we drop the penalization operator needed for the theoretical justification of convergence of the scheme); recall that $u^{\mathfrak{x},n} \in R_0^{\mathfrak{x}}$, i.e., the boundary values of $u^{\mathfrak{x},n}$ are set to be zero. The algorithm, which is a simplified version of the one of [15], follows the guidelines of Glowinski and Marrocco [36, 37]. Note that a convergence analysis of such an algorithm can be found in [15], for the more involved case of m-DDFV schemes.

We fix two parameters: $r > 0$ and $\gamma > 0$, and a tolerance threshold tol .

Initialization of the algorithm

- $k = 0$
- $u_0^{\mathfrak{x}} = u^{\mathfrak{x},n-1}$ (in the case b is not invertible, one may pick $u_0^{\mathfrak{x}} = (b + \varepsilon I)^{-1}(b^{\mathfrak{x},0})$)
- $errit = 1$
- $source = b(u^{\mathfrak{x},n-1}) + \Delta t f^{\mathfrak{x},n}$
- $g_0^{\mathfrak{x}} = \nabla^{\mathfrak{x}} u_0^{\mathfrak{x}}$
- $\lambda_0^{\mathfrak{x}} = -\varphi(\nabla^{\mathfrak{x}} u_0^{\mathfrak{x}})$.

While ($errit > tol$) **do iterations of the algorithm** $(u_{k-1}^{\mathfrak{x}}, g_{k-1}^{\mathfrak{x}}, \lambda_{k-1}^{\mathfrak{x}}) \rightarrow (u_k^{\mathfrak{x}}, g_k^{\mathfrak{x}}, \lambda_k^{\mathfrak{x}})$

- **First step** Evaluation of $u_k^{\mathfrak{x}} \in R_0^{\mathfrak{x}}$ solution of

$$b(u_k^{\mathfrak{x}}) - \Delta t \operatorname{div}^{\mathfrak{x}} (r(\nabla^{\mathfrak{x}} u_k^{\mathfrak{x}} - g_{k-1}^{\mathfrak{x}}) - \lambda_{k-1}^{\mathfrak{x}}) = source$$

or, equivalently, of

$$b(u_k^{\mathfrak{x}}) - r\Delta t \operatorname{div}^{\mathfrak{x}} (\nabla^{\mathfrak{x}} u_k^{\mathfrak{x}}) = -\Delta t \operatorname{div}^{\mathfrak{x}} (r g_{k-1}^{\mathfrak{x}} + \lambda_{k-1}^{\mathfrak{x}}) + source$$

(we can denote by $source_k$ the right-hand side of the above expression).

Thus we use the Newton method to solve this system; notice that it takes the form

$$(52) \quad b(u_k^{\bar{x}}) + r\Delta t A_0 u_k^{\bar{x}} = source_k$$

where A_0 is the matrix corresponding to the CeVe-DDFV discretization of the linear $-\Delta$ operator⁵ on the mesh \mathfrak{T} . For the sake of completeness, we write the algorithm:

– Initialization : $X^0 = u_{k-1}^{\bar{x}}$

– While $\|b(X^l) + r\Delta t A_0 X^l - source_k\| > tol$ do

$$X^{l+1} = X^l - (\text{diag } b'(X^l) + r\Delta t A_0)^{-1}(b(X^l) + r\Delta t A_0 X^l - source_k)$$

where $\text{diag } \cdot$ is the diagonal matrix with the prescribed vector \cdot of diagonal entries.

– $u_k^{\bar{x}}$ is assigned to be the final value of X^l .

- **Second step** Evaluation of $g_k^{\bar{x}} = (g_{D,k})_D \in (\mathbb{R}^{\mathfrak{D}})^3$.

Here we have $\text{card}(\mathfrak{D})$ decoupled nonlinear problems in \mathbb{R}^3 to be solved. In every diamond D we have to solve the following problem:

$$\varphi(g_{D,k}) + \lambda_{D,k-1} + r(g_{D,k} - \nabla_D u_k^{\bar{x}}) = 0$$

Once more, we use the Newton method:

– Initialization : $Y^0 = g_{D,k-1}$

– While $\|\varphi(Y^l) + \lambda_{D,k-1} + r(Y^l - \nabla_D u_k^{\bar{x}})\| > tol$ do

$$Y^{l+1} = Y^l - (D\varphi(Y^l) + rI_3)^{-1}(\varphi(Y^l) + \lambda_{D,k-1} + r(Y^l - \nabla_D u_k^{\bar{x}}))$$

where I_3 is the 3×3 identity matrix, and $D\varphi$ denotes the jacobian matrix of $\varphi : \mathbb{R}^3 \rightarrow \mathbb{R}^3$. Notice that this 3×3 system can be solved manually, offline.

– $g_{D,k}$ is assigned to be the final value of Y^l .

- **Third step** Evaluation of $\lambda_k^{\bar{x}} \in (\mathbb{R}^{\mathfrak{D}})^3$.

$$\lambda_k^{\bar{x}} = \lambda_{k-1}^{\bar{x}} + r\gamma(g_k^{\bar{x}} - \nabla^{\bar{x}} u_k^{\bar{x}})$$

- **Update of the stopping criterion.**

$$errit = \|b(u_k^{\bar{x}}) - \Delta t \text{div}^{\bar{x}} \varphi(\nabla^{\bar{x}} u_k^{\bar{x}}) - source\|.$$

End of k 'th iteration

- At the end of the iterative procedure, assign $u^{\bar{x},n}$ to be the final value $u_k^{\bar{x}}$.

REFERENCES

- [1] H.W. Alt and S. Luckhaus. Quasilinear elliptic-parabolic differential equations. *Mat. Z.* 183(1983), pp. 311–341.
- [2] B. Andreianov, M. Bendahmane, F. Hubert and S. Krell. On 3D DDFV discretization of gradient and divergence operators. I. Meshing, operators and discrete duality. *IMA J. Numer. Anal.*, to appear. Available as HAL preprint, <http://hal.archives-ouvertes.fr/hal-00355212>
- [3] B. Andreianov, M. Bendahmane, and K.H. Karlsen. Discrete duality finite volume schemes for doubly nonlinear degenerate hyperbolic-parabolic equations. *J. Hyp. Diff. Equ.* 7(2010), no.1, pp.1–67.
- [4] B. Andreianov, M. Bendahmane and K.H. Karlsen. A gradient reconstruction formula for finite volume schemes and discrete duality. In R. Eymard and J.-M. Hérard, editors, *Finite Volume For Complex Applications, Problems And Perspectives. 5th International Conference*, 161–168. London (UK) Wiley, 2008.
- [5] B. Andreianov, M. Bendahmane, K.H. Karlsen and Ch. Pierre. Convergence of Discrete Duality Finite Volume schemes for the macroscopic bidomain model of the heart electric activity. Preprint HAL, <http://hal.archives-ouvertes.fr/hal-00526047>.
- [6] B. Andreianov, M. Bendahmane and R. Ruiz Baier. Analysis of a finite volume method to solve a cross-diffusion population system. *M3AS Math. Models Meth. Appl. Sci.* 2011, DOI: 10.1142/S0218202511005064.
- [7] B. Andreianov, F. Boyer, and F. Hubert. Finite volume schemes for the p -Laplacian on Cartesian meshes. *M2AN Math. Model. Numer. Anal.* 38(6):931–959, 2004.
- [8] B. Andreianov, F. Boyer and F. Hubert. Besov regularity and new error estimates for finite volume approximations of the p -laplacian. *Numer. Math.*, 100(4):565–592, 2005.
- [9] B. Andreianov, F. Boyer and F. Hubert. On finite volume approximation of regular solutions of the p -laplacian. *IMA J. Numer. Anal.*, 26(3):472–502, 2006.

⁵In the case of non-homogeneous Dirichlet boundary condition, we still take the zero conditions for the discrete Laplace operator, and the discrete boundary condition contributes to the source term of (52))

- [10] B. Andreianov, F. Boyer, and F. Hubert. Discrete duality finite volume schemes for Leray-Lions type elliptic problems on general 2D meshes. *Numer. Meth. PDE*, 23(1):145–195, 2007.
- [11] B. Andreianov, M. Gutnic, and P. Wittbold. Convergence of finite volume approximations for a nonlinear elliptic-parabolic problem: a "continuous" approach. *SIAM J. Numer. Anal.* 42(1):228–251, 2004.
- [12] B. Andreianov, F. Hubert and S. Krell. Benchmark 3D: a version of the DDFV scheme with cell/vertex unknowns on general meshes. In *Proceedings of Finite Volumes for Complex Applications VI in Prague*, 2011, to appear.
- [13] M. Bendahmane and K.H. Karlsen. Analysis of a class of degenerate reaction-diffusion systems and the bidomain model of cardiac tissue. *Netw. Heterog. Media* 1:185–218, 2006.
- [14] M. Bendahmane and K.H. Karlsen. Convergence of a finite volume scheme for the bidomain model of cardiac tissue. *Appl. Numer. Math.*, 59(9):2266–2284, 2009.
- [15] F. Boyer and F. Hubert. Finite volume method for 2D linear and nonlinear elliptic problems with discontinuities. *SIAM J. Num. Anal.* 46(6):3032–3070, 2008.
- [16] F. Boyer, F. Hubert and S. Krell. Non-overlapping Schwarz algorithm for solving 2D-mDDFV schemes. *IMA J. Num. Anal.* 30(4):1062–1100, 2010.
- [17] Y. Coudière, Th. Gallouët and R. Herbin. Discrete Sobolev inequalities and L^p error estimates for finite volume solutions of convection diffusion equations. *M2AN Math. Model. Numer. Anal.* 35(4) (2001) 767–778.
- [18] Y. Coudière and F. Hubert. A 3D Discrete Duality Finite Volume method for nonlinear elliptic equations. In: A. Handlovičová, P. Frolkovič, K. Mikula, D. Ševčovič (Eds.), *Proceedings of Algoritmy 2009*, pp. 51–60, 2009.
- [19] Y. Coudière and F. Hubert. A 3D discrete duality finite volume method for nonlinear elliptic equation. HAL preprint 2010, <http://hal.archives-ouvertes.fr/hal-00456837>
- [20] Y. Coudière, F. Hubert and G. Manzini. Benchmark 3D: CeVeFE-DDFV, a discrete duality scheme with cell/vertex/face+edge unknowns. In *Proceedings of Finite Volumes for Complex Applications VI in Prague*, Springer, 2011, to appear.
- [21] Y. Coudière and Ch. Pierre. Benchmark 3D: CeVe-DDFV, a discrete duality scheme with cell/vertex unknowns. In *Proceedings of Finite Volumes for Complex Applications VI in Prague*, Springer, 2011, to appear.
- [22] Y. Coudière, Ch. Pierre and R. Turpault. Solving the fully coupled heart and torso problems of electrocardiology with a 3D discrete duality finite volume method. Preprint HAL 2009, <http://hal.archives-ouvertes.fr/hal-00016825>
- [23] Y. Coudière, Ch. Pierre, O. Rousseau and R. Turpault. 2D/3D discrete duality finite volume scheme. Application to ECG simulation. *Int. J. Finite Vol.* 6(1):1-24, 2009.
- [24] Y. Coudière, Ch. Pierre, O. Rousseau and R. Turpault. 2D/3D discrete duality finite volume scheme (DDFV) applied to ECG simulation. In R. Eymard and J.-M. Hérard, editors, *Finite Volume For Complex Applications, Problems And Perspectives. 5th International Conference*, 313–320. London (UK) Wiley, 2008.
- [25] K. Domelevo and P. Omnès. A finite volume method for the Laplace equation on almost arbitrary two-dimensional grids. *M2AN Math. Model. Numer. Anal.* 39(6):1203–1249, 2005.
- [26] J. Droniou. Finite volume approximations for fully nonlinear elliptic equations in divergence form. *M2AN Math. Model. Numer. Anal.* 40(6):1069–1100, 2006.
- [27] J. Droniou, T. Gallouët and R. Herbin. A finite volume scheme for a noncoercive elliptic equation with measure data. *SIAM J. Numer. Anal.* 41, no. 6, 1997–2031, 2003.
- [28] R. Eymard, T. Gallouët, and R. Herbin. Finite Volume Methods. *Handbook of Numerical Analysis*, Vol. VII, P. Ciarlet, J.-L. Lions, eds., North-Holland, 2000.
- [29] R. Eymard, T. Gallouët, and R. Herbin. Discretisation of heterogeneous and anisotropic diffusion problems on general non-conforming meshes. SUSI: a scheme using stabilisation and hybrid interfaces, *IMA J. Numer. Anal.* 30(4)1009–1043, 2010.
- [30] R. Eymard, T. Gallouët, and R. Herbin. Cell centered discretisation of non linear elliptic problems on general multidimensional polyhedral grids. *J. Numer. Math.* 17(3):173–193, 2009.
- [31] R. Eymard, T. Gallouët, R. Herbin and A. Michel. Convergence of a finite volume scheme for nonlinear degenerate parabolic equations. *Numer. Math.* 92(1):41–82, 2002.
- [32] R. Eymard, R. Herbin and C. Guichard. Small-stencil 3D schemes for diffusive flows in porous media. HAL preprint 2011, <http://hal.archives-ouvertes.fr/hal-00542667>
- [33] T. Gallouët and R. Herbin. Finite volume approximation of elliptic problems with irregular data. In: *Finite volumes for complex applications. Problems and Perspectives. II*, F. Benkhaldoun, M. Hänel and R. Vilsmeier eds, Hermès, 155–162, 1999.
- [34] T. Gallouët and J.-C. Latché. Compactness of discrete approximate solutions to parabolic pdes - application to a turbulence model. *Comm. Pure Appl. Anal.* 2011, to appear; preprint available on <http://www.cmi.univ-mrs.fr/gallouet/art.d/gl-ausid.pdf>
- [35] A. Glitzy and J.A. Griepentrog. Discrete Sobolev-Poincare inequalities for Voronoï finite volume approximations. *SIAM J. Numer. Anal.* 48(1):372–391, 2010.
- [36] R. Glowinski and A. Marrocco. Sur l'approximation, par éléments finis d'ordre un, et la résolution, par pénalisation-dualité, d'une classe de problèmes de Dirichlet non linéaires. *RAIRO Rev. Française Automat. Informat. Recherche Opérationnelle*, 9(R-2):41–76, 1975.
- [37] R. Glowinski. *Numerical methods for nonlinear variational problems*. Scientific Computation. Springer-Verlag, Berlin, 1984, 2008.

- [38] R. Herbin and F. Hubert. Benchmark on discretization schemes for anisotropic diffusion problems on general 3D grids. In *Proceedings of Finite Volumes for Complex Applications VI in Prague*, Springer, 2011, to appear.
- [39] F. Hermeline. Une méthode de volumes finis pour les équations elliptiques du second ordre. (French) *C. R. Math. Acad. Sci. Paris* 326(12):1433–1436, 1998.
- [40] F. Hermeline. A finite volume method for the approximation of diffusion operators on distorted meshes. *J. Comput. Phys.* 160(2):481–499, 2000.
- [41] F. Hermeline. Approximation of 2D and 3D diffusion operators with discontinuous full-tensor coefficients on arbitrary meshes. *Comput. Methods Appl. Mech. Engrg.*, 196(21-24):2497–2526, 2007.
- [42] F. Hermeline. A finite volume method for approximating 3D diffusion operators on general meshes. *J. Comput. Phys.* 228(16):5763–5786, 2009.
- [43] S. Krell. *Schémas Volumes Finis en mécanique des fluides complexes*. (French) Ph.D. Thesis, Univ. de Provence, Marseilles, 2010.
- [44] S.N. Kruzhkov. Results on the nature of the continuity of solutions of parabolic equations and some of their applications. *Mat. Zametki* 6(1):97–108, 1969; english tr. in *Math. Notes* 6(1):517-523, 1969.
- [45] R.A. Nicolaides. Direct discretization of planar div-curl problems. *SIAM J. Numer. Anal.*, 29:32–56, 1992.
- [46] F. Otto. L^1 contraction and uniqueness for quasilinear elliptic-parabolic equations. *J. Diff. Eq.*, 131:20–38, 1996.
- [47] Ch. Pierre. *Modélisation et simulation de l'activité électrique du coeur dans le thorax, analyse numérique et méthodes de volumes finis*. (French) Ph.D. Thesis, Université de Nantes, 2005.
- [48] L. Tung. *A bidomain model for describing ischemic myocardial D-D properties*. Ph.D. thesis, M.I.T., 1978.

BORIS ANDREIANOV, LABORATOIRE DE MATHÉMATIQUES DE BESANÇON CNRS UMR6623, UNIVERSITÉ DE FRANCHE-COMTÉ, 16 ROUTE DE GRAY, 25030 BESANÇON, FRANCE; boris.andreianov@univ-fcomte.fr

MOSTAFA BENDAHMANE, INSTITUT DE MATHÉMATIQUES DE BORDEAUX, UNIVERSITÉ VICTOR SEGALEN, 33076 BORDEAUX CEDEX, FRANCE mostafa.bendahmane@u-bordeaux2.fr

FLORENCE HUBERT, LATP, UNIVERSITÉ DE PROVENCE, 39 RUE F. JOLIOT-CURIE, 13453 MARSEILLE CEDEX 13, FRANCE; fhubert@cmi.univ-mrs.fr